Chemical Science

Synthesis and Solution-State Dynamics of Donor-Acceptor Oligorotaxane Foldamers

Zhixue Zhu,[†] Carson J. Bruns,[†,‡] Hao Li,[†] Juying Lei,[†] Chenfeng Ke,[†] Zhichang Liu,[†] Saman Shafaie,[†] Howard M. Colquhoun,[§] J. Fraser Stoddart[†,‡*]

[†]Department of Chemistry, Northwestern University, 2145 Sheridan Road, Evanston, Illinois, 60208 (USA)

[‡]NanoCentury KAIST Institute, Graduate School of Energy, Environment, Water, and Sustainability (World Class University), Korea Advanced Institute of Science and Technology (KAIST), 373-1 Guseong Dong, Yuseong Gu, Daejeon 305-701 (Republic of Korea)

[§]Department of Chemistry, University of Reading, Whiteknights, Reading, RG6 6AD (UK)

ELECTRONIC SUPPLEMENTARY INFORMATION

Table of Contents

1. General Methods

All reagents and solvents were purchased from commercial suppliers (Aldrich or Fisher) and used without further purification. Cyclobis(paraquat-*p*-phenylene) hexafluorophosphate (**CBPQT**·4PF_6),[S1] **1NPE(OTs)$_2$**,[S2] and **3NPE(OTs)$_2$**,[S3] **5NPE(OTs)$_2$**,[S3] and the stopper precursor **S1**[S4] were prepared according to literature procedures. All reactions were performed in dry solvents under a nitrogen atmosphere unless otherwise stated. Thin layer chromatography (TLC) was performed on silica gel 60 F_{254} (E. Merck) and visualized under a UV lamp at 254 nm. Column chromatography was carried out on silica gel 60F (Merck 9385, 0.040–0.063 mm). Nuclear magnetic resonance (NMR) spectra were recorded on Bruker Avance 500 and 600 spectrometers, with working frequencies of 500 and 600 MHz for ^{1}H, and 125 and 150 MHz for ^{13}C nuclei, respectively. Chemical shifts are reported in ppm and referenced to the residual non-deuterated solvents for ^{1}H ($CDCl_3$: δ = 7.26 ppm, CD_2Cl_2: δ = 5.32 ppm, CD_3CN: δ = 1.94 ppm) and ^{13}C ($CDCl_3$: δ = 77.0 ppm, CD_2Cl_2: δ = 54.0 ppm, CD_3CN: δ = 1.32 ppm). High-resolution mass spectra (HRMS) were measured in electrospray ionization (ESI) mode on Agilent 6210 LC-TOF mass spectrometer with sample introduction via an Agilent 1200 HPLC. Gel permeation chromatography (GPC) was performed using an Agilent 100 Series pump with a Viscotek ViscoGEL GPC column, coupled to a Wyatt DAWN HELEOS-II multi-angle light scattering detector and an OPTILAB rEX refractive index detector. Analyses were carried out in THF solution (5 mg·mL^{-1}) at room temperature, with a flow rate of 1.0 mL·min^{-1} and with an injection volume of 100 μL

2. Synthetic Procedures

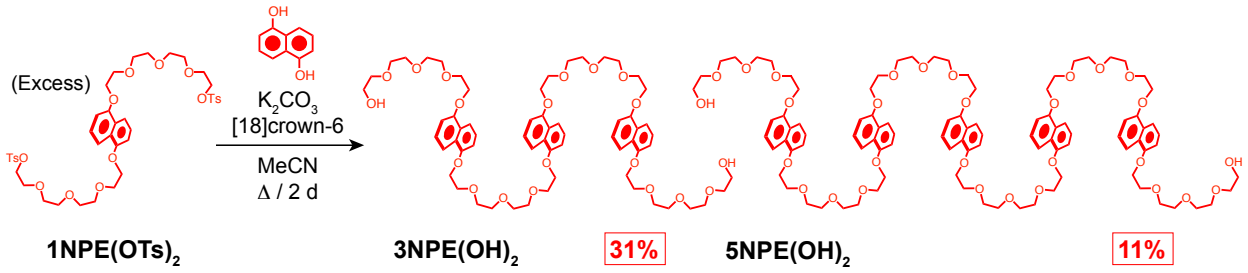

Scheme S1. One-pot synthesis of oligomers **3NPE(OH)$_2$** and **5NPE(OH)$_2$**

One-pot synthesis of oligomers 3NPE(OH)$_2$ and 5NPE(OH)$_2$: A dry round-bottomed flask was charged with 1,5-dihydroxynaphthalene (16.02 g, 100 mmol) and dry MeCN (400 mL) under a nitrogen atmosphere. K_2CO_3 (41.46 g, 300 mol) and 18-crown-6 (1.32 g, 5 mmol) were introduced and the mixture was heated under reflux for 1 h before **1NPE(OTs)$_2$** (123.1 g, 150 mmol) was added and the reaction mixture was heated under reflux for a further 48 h. The solvent was removed under reduced pressure and the reaction mixture washed with H_2O and extracted into CH_2Cl_2. The organic layers were dried (Na_2SO_4) and evaporated under reduced pressure. The residue was purified by column chromatography on SiO_2, eluting with a solvent gradient from EtOAc to EtOAc:MeOH (85:15, v/v) to afford pure **3NPE(OH)$_2$** and **5NPE(OH)$_2$**. The higher oligomers **7NPE(OH)$_2$** and **9NPE(OH)$_2$** were collected as a mixture in small quantity.

3NPE(OH)$_2$: 35.6 g, 31%; ^{1}H NMR (500 MHz, $CDCl_3$, 298 K): δ = 7.84 (d, J = 8.5 Hz, 2H), 7.83 (d, J = 8.4 Hz, 4H), 7.31 (t, J = 7.6 Hz, 2H), 7.30 (t, J = 7.6 Hz, 2H), 7.29 (t, J = 8.4 Hz, 2H), 6.80 (d, J = 7.4 Hz, 2H), 6.79 (d, J = 7.6 Hz, 2H), 6.77 (d, J = 7.7 Hz, 2H), 4.28–4.22 (m, 12H), 3.98–3.94 (m, 12H), 3.80–3.77 (m, 12H), 3.71–3.67 (m, 16H), 3.65–3.64 (m, 8H), 3.57–3.55 (m, 4H) ppm. ^{13}C NMR (125 MHz, $CDCl_3$, 298 K): δ = 160.2, 128.7, 123.6, 115.3, 105.7, 70.7, 70.4, 69.6, 62.9 ppm. HRMS (ESI-TOF-MS): *m/z* calcd for $C_{62}H_{88}NO_{20}$ $[M + NH_4]^+$: 1166.5900, found 1166.5923.

5NPE(OH)$_2$: 9.82 g, 11%; ^{1}H NMR (500 MHz, CD_2Cl_2, 298 K): δ = 7.87 (d, J = 8.2 Hz, 4H), 7.86 (d, J = 8.6 Hz, 6H), 7.39 (t, J = 8.1 Hz, 2H), 7.38 (t, J = 7.9 Hz, 4H), 7.37 (t, J = 8.1 Hz, 4H), 6.89 (d, J = 7.6 Hz, 2H), 6.87 (d, J = 7.7 Hz, 2H), 6.86 (d, J = 7.8 Hz, 6H), 4.32–4.26 (m, 20H), 4.00–3.97 (m, 20H), 3.80–3.77 (m, 20H), 3.72–3.69 (m, 24H), 3.67–3.65 (m, 8H), 3.58–3.56 (m, 4H) ppm. ^{13}C NMR (125 MHz, $CDCl_3$, 298 K): δ = 154.7, 127.0, 125.6, 115.7, 106.0, 72.8, 71.3, 71.0, 70.7, 70.1, 68.4, 62.0 ppm. HRMS (ESI-TOF-MS): *m/z* calcd for $C_{98}H_{132}NO_{30}$ $[M + NH_4]^+$: 1802.8834, found 1802.8817.

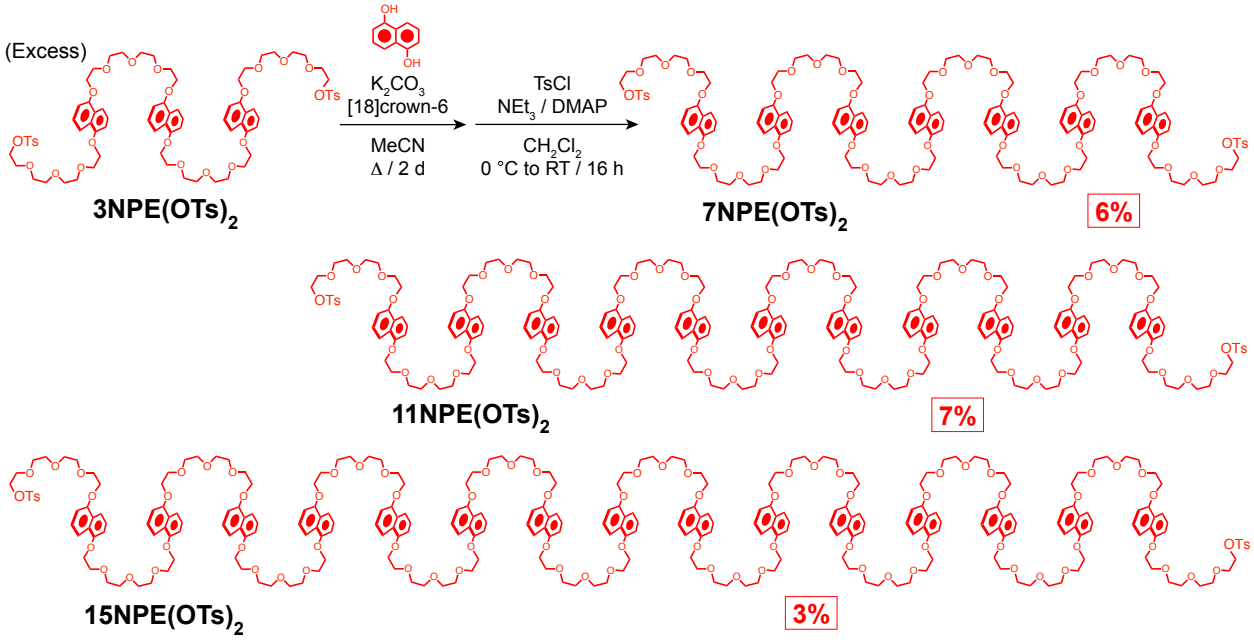

Scheme S2. One-pot synthesis of extended DNP oligomers **7NPE(OTs)$_2$**, **11NPE(OTs)$_2$**, and **15NPE(OTs)$_2$**

One-pot synthesis of oligomers 7NPE(OTs)$_2$, 11NPE(OTs)$_2$, and 15NPE(OTs)$_2$: A dry round-bottomed flask was charged with 1,5-dihydroxynaphthalene (733 mg, 4.57 mol) and dry MeCN (200 mL) under a nitrogen atmosphere. K_2CO_3 (1.898 g, 13.72 mol) and 18-crown-6 (80 mg, 0.3 mmol) were added and the mixture was heated under reflux for 1 h before **3NPE(OTs)$_2$** (10.0 g, 6.86 mmol) was added and the reaction mixture was heated under reflux for a further 48 h. The solvent was removed under reduced pressure and the reaction mixture was washed with H_2O and extracted into CH_2Cl_2. The organic layers were dried (Na_2SO_4) and the solvent was removed under reduced pressure. The crude product (2 g) was taken up in dry CH_2Cl_2 (50 mL) and Et_3N (526 mg, 0.725 mL, 5.2 mmol) and 4-dimethylaminopyridine (DMAP) (21 mg, 0.17 mmol) were added at 0 °C under a nitrogen atmosphere. After 5 min, a solution of *p*-toluenesulfonyl chloride (TsCl) (827 mg, 4.33 mmol) in CH_2Cl_2 (5 mL) was added directly to the reaction vessel. The reaction mixture was allowed to warm up to ambient temperature and it was stirred for an additional 16 h. The mixture was concentrated under reduced pressure, washed with H_2O, extracted into CH_2Cl_2, dried (Na_2SO_4), filtered, concentrated under reduced pressure, and purified by column chromatography on SiO_2, eluting with a solvent gradient from EtOAc to MeOH:EtOAc (1:4 v/v), to afford the individual products as colorless solids.

7NPE(OTs)$_2$: 700 mg, 6%; ^{1}H NMR (500 MHz, CD_2Cl_2, 298 K): δ = 7.90–7.86 (m, 14H), 7.80 (d, J = 8.4 Hz, 4H), 7.41–7.39 (m, 18H), 6.90–6.85 (m, 14H), 4.31–4.26 (m, 28H), 4.14–4.12 (m, 4H), 4.00–3.96 (m, 28H), 3.80–3.76 (m, 28H), 3.73–3.70 (m, 24H), 3.67–3.64 (m, 8H), 3.61–3.59 (m, 4H), 3.58–3.56 (m, 4H), 2.45 (s, 6H) ppm. ^{13}C NMR (125 MHz, CD_2Cl_2, 298 K): δ = 154.8, 151.9, 145.5, 136.2, 133.2, 130.3, 128.7, 128.3, 127.0, 125.8, 125.6, 114.7, 106.3, 106.0, 71.3, 71.2, 71.0, 70.8, 70.1, 69.9, 69.0, 68.4, 30.5 ppm. HRMS (ESI-TOF-MS): *m/z* calcd for $C_{148}H_{192}N_2O_{44}S_2$ $[M + 2NH_4]^+$: 1382.6164, found 1382.6164; *m/z* calcd for $C_{148}H_{196}N_3O_{44}S_2$ $[M + 3NH_4]^+$: 927.7526, found 927.7584.

11NPE(OTs)$_2$: 640 mg, 7%; ^{1}H NMR (500 MHz, CD_2Cl_2, 298 K): δ = 7.90–7.86 (m, 22H), 7.80 (d, J = 8.3 Hz, 4H), 7.41–7.36 (m, 26H), 6.89 – 6.85 (m, 22H), 4.30–4.26 (m, 44H), 4.14–4.12 (m, 4H), 4.00–3.96 (m, 44H), 3.80–3.76 (m, 44H), 3.73–3.70 (m, 40H), 3.67–3.64 (m, 8H), 3.61–3.58 (m, 4H), 3.57–3.55 (m, 4H), 2.45 (s, 6H) ppm. ^{13}C NMR (125 MHz, CD_2Cl_2, 298 K): δ = 154.7, 151.9, 145.5, 136.2, 133.2, 130.3, 128.7, 128.3, 127.0, 125.8, 125.6, 114.7, 108.3, 106.0, 71.3, 71.0, 70.8, 70.1, 69.9, 69.4, 69.0, 68.4, 68.0, 64.0, 30.5 ppm. HRMS (ESI-TOF-MS): *m/z* calcd for $C_{220}H_{280}N_2O_{64}S_2$ $[M + 2NH_4]^{2+}$: 2018.9019, found 2018.8994; *m/z* calcd for $C_{220}H_{284}N_3O_{64}S_2$ $[M + 3NH_4]^{3+}$: 1351.9501, found 1351.9486; *m/z* calcd for $C_{220}H_{288}N_4O_{64}S_2$ $[M + 4NH_4]^{4+}$: 1018.4712, found 1018.4687.

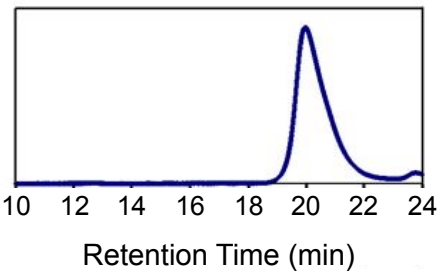

Figure S1. GPC trace of **11NPE(OTs)$_2$**. M_n = 4.49 x 10^3, M_w = 4.54 x 10^3, PDI = 1.01

15NPE(OTs)$_2$: 240 mg, 3%; ^{1}H NMR (500 MHz, CD_2Cl_2, 298 K): δ = 7.89–7.86 (m, 30H), 7.79 (d, J = 8.3 Hz, 4H), 7.40–7.35 (m, 34H), 6.88 (d, J = 8.3 Hz, 4H), 6.87–6.84 (m, 30H), 4.30–4.25 (m, 60H), 4.13–4.11 (m, 4H), 3.99–3.96 (m, 60H), 3.80–3.76 (m, 60H), 3.72–3.68 (m, 56H), 3.66–3.64 (m, 8H), 3.60–3.58 (m, 4H), 3.57–3.55 (m, 4H), 2.45 (s, 6H) ppm. ^{13}C NMR (125 MHz, CD_2Cl_2, 298 K): δ = 154.7, 151.8, 145.5, 136.2, 133.2, 130.3, 128.7, 128.3, 127.0, 125.8,

125.6, 114.7, 106.0, 71.3, 71.0, 70.8, 70.1, 69.9, 68.9, 68.4, 30.5 ppm. HRMS (ESI-TOF-MS): *m/z* calcd for $C_{292}H_{368}N_2O_{84}S_2$ $[M + 2NH_4]^{2+}$: 2655.2014, found 2655.2017; *m/z* calcd for $C_{292}H_{372}N_3O_{84}S_2$ $[M + 3NH_4]^{3+}$: 1776.1457, found 1776.1505; *m/z* calcd for $C_{292}H_{376}N_4O_{84}S_2$ $[M + 4NH_4]^{4+}$: 1336.6179, found 1336.6213; *m/z* calcd for $C_{292}H_{380}N_5O_{84}S_2$ $[M + 5NH_4]^{5+}$: 1072.9012, found 1072.8850.

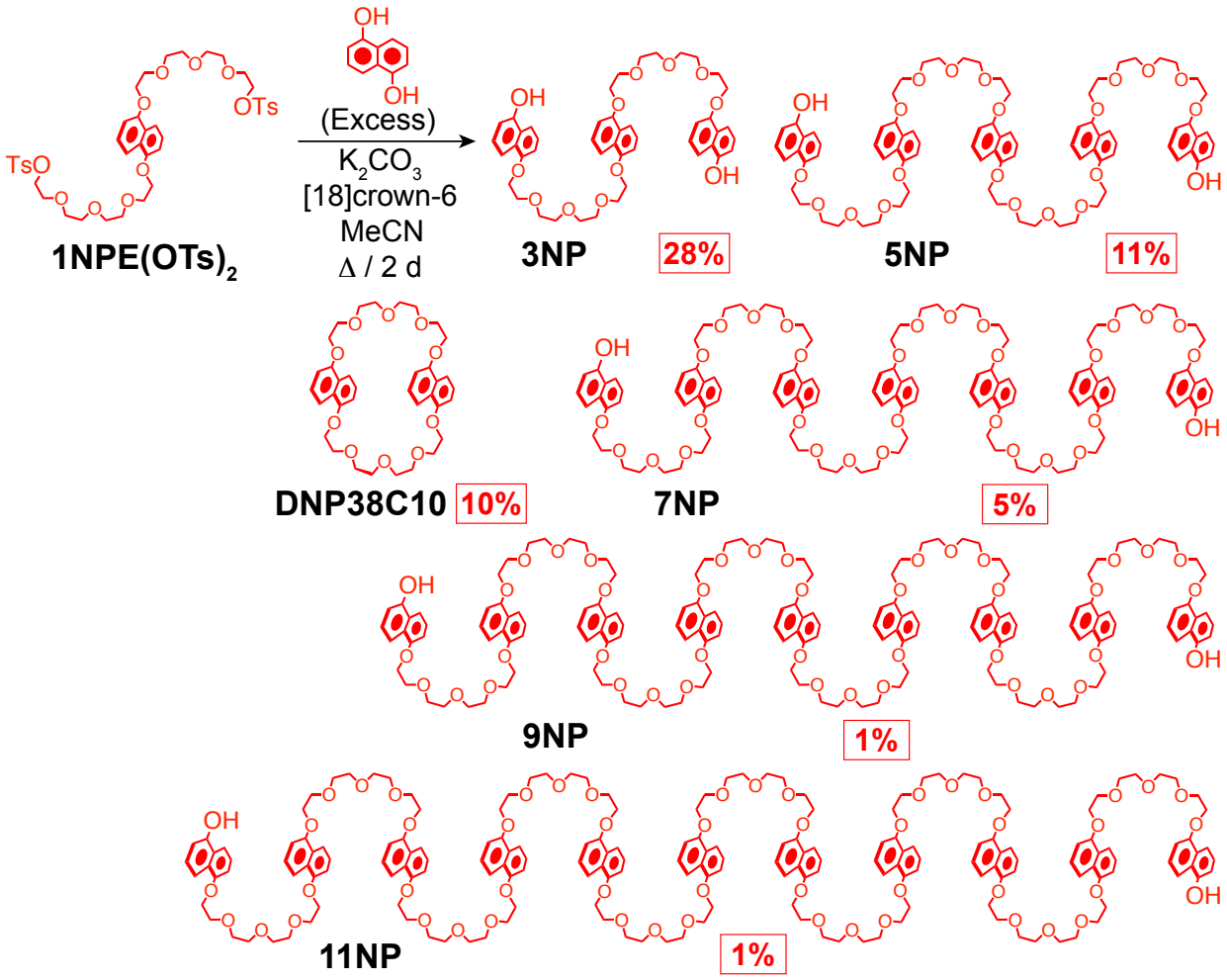

Scheme S3. Synthesis of DNP oligomers

One-pot synthesis of oligomers (3NP, 5NP, 7NP, 9NP, 11NP): A dry round-bottomed flask was charged with 1,5-dihydroxynaphthalene (24.02 g, 150 mol) and dry MeCN (800 mL) under a nitrogen atmosphere. K_2CO_3 (20.73 g, 150 mol) and 18-crown-6 (2.643 g, 10 mmol) were added and the mixture was heated under reflux for 1 h before **1NPE(OTs)$_2$** (41.05 g, 50 mol) was added and the reaction mixture was heated under reflux for a further 48 h. The reaction

mixture was concentrated under reduced pressure, washed with H_2O, and extracted into CH_2Cl_2. The organic layers were dried (Na_2SO_4) and concentrated under reduced pressure. The crude material was purified on SiO_2, eluting with a solvent gradient from hexane:EtOAc (4:1 v/v) to EtOAc to obtain a crystalline solid, identified as **DNP38C10** (1.65 g, 10%). Continued elution in a gradient from EtOAc to MeOH:EtOAc (15:85 v/v) afforded **3NP**, **5NP**, **7NP**, **9NP**, and **11NP** as viscous liquids. Some impure fractions were subjected to repeated purification as described above.

3NP: 10.6 g, 28%; ^{1}H NMR (500 MHz, $CDCl_3$, 298 K): δ = 7.82 (d, J = 8.5 Hz, 2H), 7.77 (d, J = 8.3 Hz, 2H), 7.76 (d, J = 7.2 Hz, 2H), 7.30 (d, J = 8.3 Hz, 2H), 7.25 (d, J = 8.2 Hz, 2H), 7.12 (d, J = 8.3 Hz, 2H), 6.81 (d, J = 7.5 Hz, 2H), 6.73 (d, J = 7.6 Hz, 2H), 6.66 (d, J = 7.7 Hz, 2H), 4.22–4.20 (m, 4H), 4.19–4.17 (m, 4H), 3.97–3.96 (m, 4H), 3.95–3.94 (m, 4H), 3.83–3.79 (m, 4H), 3.77–3.76 (m, 4H) ppm. ^{13}C NMR (125 MHz, $CDCl_3$, 298 K): δ = 154.3, 154.2, 152.3, 127.0, 126.7, 125.8, 125.3, 125.1, 124.8, 114.5, 114.4, 109.2, 105.6, 105.3, 70.9, 70.8, 70.7, 69.8, 69.7, 68.0, 67.7, 67.6 ppm. HRMS (ESI-TOF-MS): *m/z* calcd for $C_{46}H_{53}O_{12}$ $[M + H]^+$: 797.3532, found 797.3505.

5NP: 3.34 g, 11%; ^{1}H NMR (500 MHz, $CDCl_3$, 298 K): δ = 7.87–7.83 (m, 8H), 7.76 (d, J = 8.4 Hz, 2H), 7.32–7.27 (m, 8H), 7.18 (t, J = 7.9 Hz, 2H), 6.90 (d, J = 7.4 Hz, 2H), 6.76–6.71 (m, 6H), 6.70 (d, J = 7.6 Hz, 2H), 4.22–4.17 (m, 16H), 3.95–3.92 (m, 16H), 3.80–3.77 (m, 16H), 3.73–3.71 (m, 16H) ppm. ^{13}C NMR (125 MHz, $CDCl_3$, 298 K): δ = 154.3, 154.2, 152.5, 127.0, 126.7, 125.9, 125.4, 125.1, 125.0, 124.6, 114.6, 114.5, 113.6, 109.2, 105.6, 105.3, 71.0, 70.9, 70.7, 69.8, 69.7, 67.8, 67.7 ppm. HRMS (ESI-TOF-MS): *m/z* calcd for $C_{82}H_{97}O_{22}$ $[M + H]^+$: 1433.6471, found 1433.6456.

7NP: 1.6 g, 5%; ^{1}H NMR (500 MHz, $CDCl_3$, 298 K): δ = 7.87–7.83 (m, 10H), 7.78 (d, J = 8.9 Hz, 2H), 7.76 (d, J = 8.9 Hz, 2H), 7.33–7.29 (m, 10H), 7.26 (t, J = 7.9 Hz, 2H), 7.12 (t, J = 7.9 Hz, 2H), 6.82 (d, J = 7.6 Hz, 2H), 6.78–6.75 (m, 10H), 6.65 (d, J = 7.6 Hz, 2H), 4.25–4.21 (m, 20H), 4.19–4.17 (m, 4H), 3.97–3.94 (m, 24H), 3.82–3.77 (m, 24H), 3.75–3.72 (m, 24H) ppm. ^{13}C NMR (125 MHz, $CDCl_3$, 298 K): δ = 154.3, 152.4, 127.0, 126.7, 125.8, 125.3, 125.1, 124.7, 114.6, 113.7, 109.2, 105.6, 105.3, 71.0, 70.9, 70.8, 69.8, 68.0, 67.9, 67.8, 67.7 ppm. HRMS

(ESI-TOF-MS): *m/z* calcd for $C_{118}H_{144}NO_{32}$ $[M + NH_4]^+$: 2086.9666, found 2086.9665; *m/z* calcd for $C_{118}H_{140}NaO_{32}$ $[M + Na]^+$: 2091.9225, found 2091.9264.

9NP: 600 mg, 1%; ^{1}H NMR (500 MHz, $CDCl_3$, 298 K): δ = 7.88–7.84 (m, 12H), 7.80 (d, J = 8.5 Hz, 2H), 7.76 (d, J = 8.5 Hz, 2H), 7.34–7.26 (m, 14H), 7.13 (t, J = 8.2 Hz, 2H), 6.85 (d, J = 7.6 Hz, 2H), 6.78–6.75 (m, 12H), 6.68 (d, J = 7.6 Hz, 2H), 4.24–4.21 (m, 28H), 4.19–4.17 (m, 4H), 3.97–3.95 (m, 32H), 3.81–3.79 (m, 32H), 3.75–3.72 (m, 32H) ppm. ^{13}C NMR (125 MHz, $CDCl_3$, 298 K): δ = 154.4, 154.3, 154.2, 152.3, 127.0, 126.7, 125.8, 125.3, 125.1, 124.7, 114.6, 113.8, 109.3, 105.6, 105.3, 71.0, 70.9, 70.8, 69.8, 68.0, 67.9, 67.8, 67.7 ppm. HRMS (ESI-TOF-MS): *m/z* calcd for $C_{154}H_{188}NO_{42}$ $[M + NH_4]^+$: 2723.2706, found 2723.2702; *m/z* calcd for $C_{154}H_{184}NaO_{42}$ $[M + Na]^+$: 2728.2160, found 2728.2228.

11NP: 400 mg, 1%; ^{1}H NMR (500 MHz, $CDCl_3$, 298 K): δ = 7.89–7.85 (m, 18H), 7.82 (d, J = 8.5 Hz, 2H), 7.77 (d, J = 8.4 Hz, 2H), 7.35–7.27 (m, 20H), 7.15 (t, J = 8.2 Hz, 2H), 6.87 (d, J = 7.4 Hz, 2H), 6.79–6.74 (m, 18H), 6.69 (d, J = 7.6 Hz, 2H), 4.24–4.18 (m, 36H), 3.98–3.93 (m, 36H), 3.82–3.78 (m, 36H), 3.75–3.72 (m, 36H) ppm. ^{13}C NMR (125 MHz, $CDCl_3$, 298 K): δ = 154.4, 154.3, 154.2, 152.2, 135.8, 127.0, 126.7, 125.8, 125.6, 125.3, 125.1, 124.7, 114.6, 114.5, 113.8, 109.3, 105.6, 105.3, 71.0, 70.8, 69.8, 68.0, 67.9, 67.8, 67.7 ppm. HRMS (ESI-TOF-MS): *m/z* calcd for $C_{190}H_{232}NO_{52}$ $[M + NH_4]^+$: 3359.5540, found 3359.6126; *m/z* calcd for $C_{190}H_{228}NaO_{52}$ $[M + Na]^+$: 3364.5094, found 3364.5409.

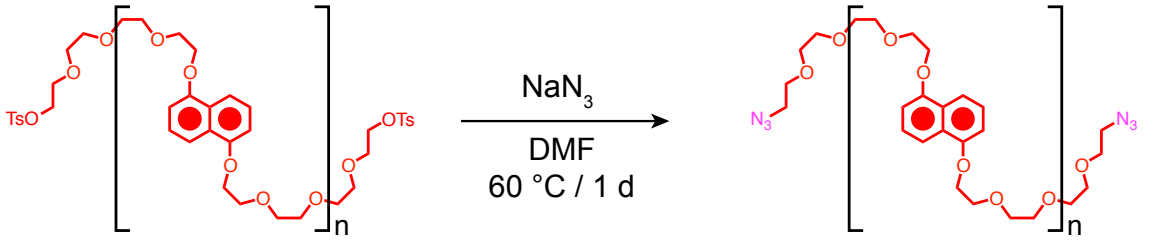

	n
1NPE(OTs)$_2$	1
3NPE(OTs)$_2$	3
5NPE(OTs)$_2$	5
7NPE(OTs)$_2$	7
11NPE(OTs)$_2$	11
15NPE(OTs)$_2$	15

	n	%
1NPE(N$_3$)$_2$	1	96
3NPE(N$_3$)$_2$	3	92
5NPE(N$_3$)$_2$	5	94
7NPE(N$_3$)$_2$	7	90
11NPE(N$_3$)$_2$	11	92
15NPE(N$_3$)$_2$	15	92

Scheme S4. Synthesis of oligomeric DNP diazides

General procedure for the synthesis of the diazides: The synthesis of **7NPE(N$_3$)$_2$** is given as a representative example. A mixture of **7NPE(OTs)$_2$** (400 mg, 0.147 mmol) and sodium azide (28.6 mg, 0.44 mmol) in DMF (30 mL) was heated at 60 °C overnight. The solvent was removed under reduced pressure and the reaction mixture was washed with H_2O and extracted into CH_2Cl_2. The organic layers were dried ($MgSO_4$), concentrated under reduced pressure, and chromatographed on SiO_2, eluting with a solvent gradient from CH_2Cl_2 to CH_2Cl_2:MeOH (85:15 v/v) to afford the diazide **7NPE(N$_3$)$_2$** as a pale yellow solid (326 mg, 90%).

1NPE(N$_3$)$_2$: 2.26 g, 96%; ^{1}H NMR (500 MHz, $CDCl_3$, 298 K): δ = 7.85 (d, J = 8.5 Hz, 2H), 7.34 (t, J = 8.5 Hz, 2H), 6.83 (d, J = 8.5 Hz, 2H), 4.29 (t, J = 4.7 Hz, 4H), 4.00 (t, J = 5.0 Hz, 4H), 3.82–3.80 (m, 4H), 3.72–3.68 (m, 8H), 3.66–3.63 (m, 8H), 3.35 (t, J = 5.2 Hz, 4H) ppm. ^{13}C NMR (125 MHz, $CDCl_3$, 298 K): δ = 154.3, 126.7, 125.1, 114.6, 105.6, 71.0, 70.8, 70.7, 70.0, 69.8, 67.9, 50.7 ppm. HRMS (ESI-TOF-MS): *m/z* calcd for $C_{26}H_{39}N_6O_8$ $[M + H]^+$: 563.2829, found 563.2789.

3NPE(N$_3$)$_2$: 3.31 g, 92%; ^{1}H NMR (500 MHz, $CDCl_3$, 298 K): δ = 7.85 (d, J = 8.4 Hz, 2H), 7.84 (d, J = 8.4 Hz, 4H), 7.33 (t, J = 8.4 Hz, 2H), 7.31 (t, J = 8.4 Hz, 4H), 6.81 (d, J = 8.4 Hz, 2H), 6.80 (d, J = 8.4 Hz, 2H), 6.78 (d, J = 8.4 Hz, 2H), 4.29–4.24 (m, 12H), 4.00–3.96 (m, 12H), 3.73–3.63 (m, 24H), 3.34 (t, J = 5.2 Hz, 4H) ppm. ^{13}C NMR (125 MHz, $CDCl_3$, 298 K): δ = 154.3, 126.7, 125.1, 114.6, 105.6, 71.0, 70.8, 70.7, 70.0, 69.8, 67.9, 50.7 ppm. HRMS (ESI-TOF-MS): *m/z* calcd for $C_{62}H_{83}N_6O_{18}$ $[M + H]^+$: 1199.5764, found 1199.5718.

5NPE(N$_3$)$_2$: 1.71 g, 94%; ^{1}H NMR (600 MHz, $CDCl_3$, 298 K): δ = 7.87 (d, J = 8.5 Hz, 2H), 7.86 (d, J = 8.5 Hz, 8H), 7.36 (t, J = 8.5 Hz, 2H), 7.35 (t, J = 8.5 Hz, 2H), 7.34 (t, J = 8.5 Hz, 6H), 6.81 (d, J = 8.5 Hz, 2H), 6.80 (d, J = 8.5 Hz, 2H), 6.78 (d, J = 8.5 Hz, 6H), 4.29–4.23 (m, 20H), 4.01–3.97 (m, 20H), 3.83–3.81 (m, 20H), 3.75–3.72 (m, 20H), 3.71–3.69 (m, 4H), 3.67–3.64 (m, 8H), 3.37 (t, J = 5.1 Hz, 4H) ppm. ^{13}C NMR (125 MHz, $CDCl_3$, 298 K): δ = 154.3, 126.7, 125.1,

114.6, 105.6, 71.0, 70.9, 70.7, 70.0, 69.8, 67.9, 50.6 ppm. HRMS (ESI-TOF-MS): *m/z* calcd for $C_{98}H_{130}N_7O_{28}$ $[M + NH_4]^+$: 1852.8964, found 1852.8948; *m/z* calcd for $C_{98}H_{134}N_8O_{28}S_4$ $[M + 2NH_4]^{2+}$ 935.4654, found 935.4519.

7NPE(N$_3$)$_2$: 310 mg, 90%; ^{1}H NMR (500 MHz, CD_2Cl_2, 298 K): δ = 7.88 (d, J = 8.4 Hz, 14H), 7.40 (t, J = 8.4 Hz, 4H), 7.38 (t, J = 8.4 Hz, 10H), 6.89 (d, J = 8.4 Hz, 2H), 6.88 (d, J = 8.4 Hz, 2H), 6.86 (d, J = 8.4 Hz, 10H), 4.31–4.27 (m, 28H), 4.00–3.97 (m, 28H), 3.79–3.78 (m, 28H), 3.74–3.69 (m, 28H), 3.67–3.65 (m, 12H), 3.38 (t, J = 5.0 Hz, 4H) ppm. ^{13}C NMR (125 MHz, CD_2Cl_2, 298 K): δ = 154.8, 127.1, 125.6, 114.8, 106.0, 71.3, 71.1, 71.0, 70.3, 70.1, 68.4, 68.2, 67.9, 51.2 ppm. HRMS (ESI-TOF-MS): *m/z* calcd for $C_{134}H_{178}N_8O_{38}$ $[M + 2NH_4]^{2+}$: 1253.6116, found 1253.6072.

11NPE(N$_3$)$_2$: 250 mg, 92%; ^{1}H NMR (500 MHz, CD_2Cl_2, 298 K): δ = 7.89 (d, J = 8.4 Hz, 22H), 7.40 (t, J = 8.4 Hz, 4H), 7.38 (t, J = 8.4 Hz, 18H), 6.89 (d, J = 8.4 Hz, 2H), 6.88 (d, J = 8.4 Hz, 2H), 6.86 (d, J = 8.4 Hz, 18H), 4.31–4.27 (m, 44H), 4.00–3.97 (m, 44H), 3.79–3.77 (m, 44H), 3.72–3.69 (m, 44H), 3.67–3.64 (m, 12H), 3.38 (t, J = 5.0 Hz, 4H) ppm. ^{13}C NMR (125 MHz, CD_2Cl_2, 298 K): δ = 154.8, 127.0, 125.6, 114.7, 106.0, 71.3, 71.0, 70.3, 70.1, 68.4, 51.2 ppm. HRMS (ESI-TOF-MS): *m/z* calcd for $C_{206}H_{266}N_8O_{58}$ $[M + 2NH_4]^{2+}$: 1889.9055, found 1889.9040.

15NPE(N$_3$)$_2$: 250 mg, 92%; ^{1}H NMR (500 MHz, CD_2Cl_2, 298 K): δ = 7.88 (d, J = 8.4 Hz, 30H), 7.40 (t, J = 8.4 Hz, 4H), 7.38 (t, J = 8.4 Hz, 26H), 6.89 (d, J = 8.4 Hz, 2H), 6.88 (d, J = 8.4 Hz, 2H), 6.86 (d, J = 8.4 Hz, 26H), 4.31–4.27 (m, 60H), 4.00–3.97 (m, 60H), 3.79–3.77 (m, 60H), 3.72–3.69 (m, 60H), 3.67–3.65 (m, 12H), 3.38 (t, J = 5.1 Hz, 4H) ppm. ^{13}C NMR (125 MHz, CD_2Cl_2, 298 K): δ = 154.8, 127.1, 125.6, 114.8, 106.0, 71.3, 71.1, 71.0, 70.3, 70.1, 68.4, 68.2, 51.2 ppm. HRMS (ESI-TOF-MS): *m/z* calcd for $C_{278}H_{354}N_8O_{78}$ $[M + 2NH_4]^{2+}$: 2526.1990, found 2526.1945; *m/z* calcd for $C_{278}H_{358}N_9O_{78}$ $[M + 3NH_4]^{3+}$: 1690.1441, found 1690.1493; *m/z* calcd for $C_{278}H_{362}N_{10}O_{78}$ $[M + 4NH_4]^{4+}$: 1272.1166, found 1272.1182.

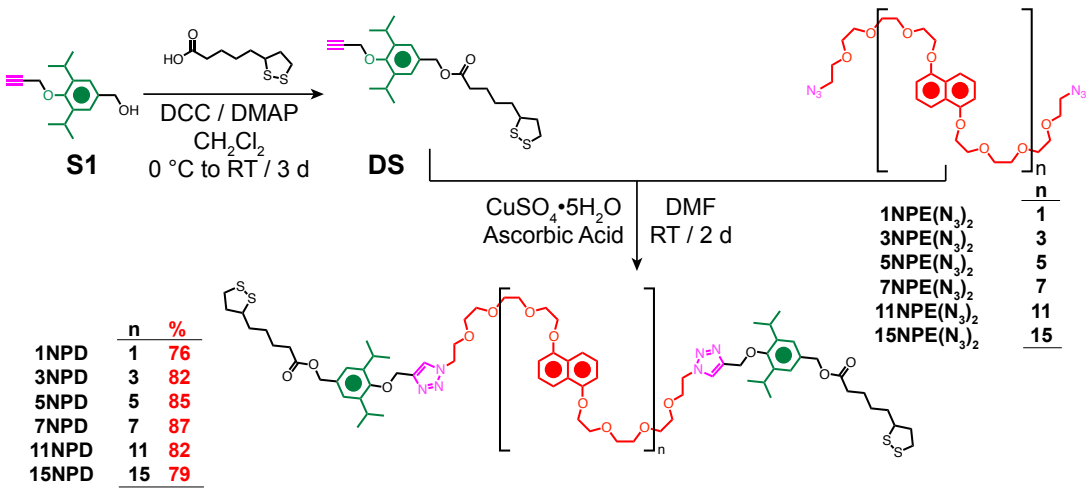

Scheme S5. Synthesis of oligomeric DNP dumbbells

Synthesis of dithiolane stopper DS. A mixture of the stopper precursor **S1** (360 mg, 1.46 mmol) and thioctic acid (453 mg, 2.2 mmol) was stirred for 15 min at 0 °C in CH_2Cl_2 (50 mL) and DCC (604 mg, 2.93 mmol) and DMAP (54 mg, 0.44 mmol) were added. The mixture was stirred at room temperature over 3 d before filtering off a white precipitate. The filtrate was concentrated and purified by column chromatography on SiO_2 in CH_2Cl_2:hexanes (1:1 v/v) to afford stopper **DS** as yellow oil (630 mg, 99%). ^{1}H NMR (500 MHz, $CDCl_3$, 298 K): δ = 7.10 (s, 2H), 5.07 (s, 2H), 4.47 (s, 2H), 3.66–3.60 (m, 1H), 3.42–3.37 (m, 2H), 3.21–3.09 (m, 2H), 2.59 (t, J = 2.3 Hz, 1H), 2.49–2.43 (m, 1H), 2.40 (t, J = 7.4 Hz, 2H), 1.94–1.88 (m, 1H), 1.76–1.67 (m, 4H), 1.54–1.45 (m, 2H), 1.25 (d, J = 7.0 Hz, 12H) ppm. ^{13}C NMR (125 MHz, $CDCl_3$, 298 K): δ =173.4, 152.7, 142.2, 132.6, 124.4, 79.1, 75.3, 66.4, 62.0, 56.3, 40.2, 38.5, 34.6, 34.1, 28.8, 26.8, 24.7, 24.1 ppm. HRMS (ESI-TOF-MS): *m/z* calcd for $C_{24}H_{34}NaO_3S_2$ $[M + Na]^+$: 457.1847, found 457.1853.

General procedure for the synthesis of dumbbells: The synthesis of dumbbell **7NPD** is given as a representative example. A mixture of **11NPE(N$_3$)$_2$** (21.5 mg, 0.006 mmol), the alkyne stopper **DS** (10.7 mg, 0.025 mmol), and ascorbic acid (4.35 mg, 0.025 mmol) in DMF (6 mL) was stirred at room temperature for 1 h, then $CuSO_4 \cdot 5H_2O$ (3.0 mg, 0.013 mmol) was added and the reaction stirred at room temperature for 2 d. The solvent was evaporated under reduced pressure, washed with H_2O, extracted into CH_2Cl_2, dried ($MgSO_4$), concentrated, and purified by column chromatography on SiO_2, eluting with a solvent gradient from neat CH_2Cl_2 to CH_2Cl_2:MeOH (85:15 v/v) to afford the product.

1NPD: 54 mg (0.048 mmol scale), 76%; ^{1}H NMR (600 MHz, CD_2Cl_2, 298 K): δ = 7.84 (s, 2H), 7.82 (d, J = 8.4 Hz, 2H), 7.33 (t, J = 8.0 Hz, 2H), 7.11 (s, 4H), 6.85 (d, J = 7.6 Hz, 2H), 5.04 (s, 4H), 4.89 (s, 4H), 4.52 (t, J = 5.1 Hz, 4H), 4.27–4.25 (m, 4H), 3.95–3.93 (m, 4H), 3.87–3.85 (m, 4H), 3.75–3.73 (m, 4H), 3.65–3.63 (m, 4H), 3.62–3.60 (m, 8H), 3.56 (tt, J = 6.3, 8.4 Hz, 2H), 3.43 (hept, J = 7.0 Hz, 4H), 3.16 (dt, J = 7.0, 12.0 Hz, 2H), 3.09 (dt, J = 7.0, 11.0 Hz, 2H), 2.46–2.41 (m, 2H), 2.37 (t, J = 7.5 Hz, 4H), 1.91–1.85 (m, 2H), 1.73–1.62 (m, 8H), 1.52–1.42 (m, 4H), 1.22 (d, J = 6.9 Hz, 24H) ppm. ^{13}C NMR (125 MHz, CD_2Cl_2, 298 K): δ = 173.7, 154.8, 153.4, 144.6, 142.7, 133.1, 127.1, 125.7, 124.8, 124.3, 114.9, 106.2, 71.4, 71.1, 70.9, 70.3, 70.0, 68.6, 68.5, 66.8, 56.9, 50.8, 40.8, 39.0, 35.1, 34.6, 29.3, 27.2, 25.3, 24.3 ppm. HRMS (ESI-TOF-MS): *m/z* calcd for $C_{74}H_{107}N_6O_{14}S_4$ $[M + H]^+$ 1431.6728, found 1431.6693; *m/z* calcd for $C_{74}H_{106}N_6NaO_{14}S_4$ $[M + Na]^+$ 1453.6548, found 1453.6538.

3NPD: 45 mg (0.025 mmol scale), 82%; ^{1}H NMR (600 MHz, CD_2Cl_2, 298 K): δ = 7.86–7.82 (m, 8H), 7.35–7.32 (m, 6H), 7.11 (s, 4H), 6.85–6.83 (m, 6H), 5.05 (s, 4H), 4.90 (s, 4H), 4.51 (t, J = 5.0 Hz, 4H), 4.27–4.23 (m, 12H), 4.96–4.92 (m, 12H), 3.86 (t, J = 5.0 Hz, 4H), 3.76–3.73 m, 12H), 3.69–3.66 (m, 12H), 3.65–3.62 (m, 4H), 3.61–3.60 (m, 8H), 3.56 (tt, J = 6.3, 8.4 Hz, 2H), 3.41 (hept, J = 7.0 Hz, 4H), 3.16 (dt, J = 7.0, 12.0 Hz, 2H), 3.08 (dt, J = 7.0, 11.0 Hz, 2H), 2.46–2.41 (m, 2H), 2.37 (t, J = 7.5 Hz, 4H), 1.91–1.85 (m, 2H), 1.73–1.62 (m, 8H), 1.52–1.42 (m, 4H), 1.22 (d, J = 6.9 Hz, 24H) ppm. ^{13}C NMR (125 MHz, CD_2Cl_2, 298 K): δ = 173.7, 154.9, 154.8, 154.8, 153.4, 144.6, 142.7, 133.1, 129.6, 129.5, 129.0, 128.6, 128.4, 127.1, 127.1, 125.7, 124.8, 114.9, 114.8, 114.7, 106.1, 71.4, 71.2, 71.1, 71.1, 71.0, 70.2, 69.9, 68.6, 68.5, 68.4, 66.8, 56.9, 50.8, 40.7, 39.0, 35.1, 34.5, 29.3, 27.1, 25.2, 24.3 ppm. HRMS (ESI-TOF-MS): *m/z* calcd for $C_{110}H_{151}N_6O_{24}S_4$ $[M + H]^+$ 2067.9657, found 2067.9667; *m/z* calcd for $C_{110}H_{152}N_6O_{24}S_4$ $[M + 2H]^+$ 1034.4865, found 1034.4890.

5NPD: 39 mg, 85%; ^{1}H NMR (600 MHz, CD_2Cl_2, 298 K): δ = 7.86–7.83 (m, 10H), 7.37–7.34 (m, 10H), 7.12 (s, 4H), 6.97 (s, 2H), 6.86–6.83 (m, 10H), 5.05 (s, 4H), 4.90 (s, 4H), 4.52 (t, J = 5.0 Hz, 4H), 4.27–4.25 (m, 20H), 3.96–3.94 (m, 20H), 3.87 (t, J = 5.0 Hz, 4H), 3.77–3.74 (m, 20H), 3.69–3.68 (m, 16H), 3.65–3.64 (m, 4H), 3.62 (br s, 8H), 3.58–3.54 (m, 2H), 3.44–3.37 (m, 4H), 3.19–3.15 (m, 2H), 3.13–3.08 (m, 2H), 2.47–2.42 (m, 2H), 2.38 (t, J = 5.0 Hz, 4H), 1.92–1.87 (m, 2H), 1.74–1.64 (m, 8H), 1.53–1.45 (m, 4H), 1.24 (d, J = 6.9 Hz, 24H) ppm. ^{13}C NMR

(125 MHz, CD_2Cl_2, 298 K): δ = 173.6, 154.7, 153.3, 151.9, 144.5, 142.6, 136.2, 133.0, 128.7, 127.0, 125.8, 125.6, 124.7, 124.6, 124.2, 114.7, 106.0, 71.3, 71.0, 70.9, 70.1, 69.8, 68.5, 68.4, 68.2, 66.7, 62.3, 56.8, 50.7, 40.6, 38.9, 35.0, 34.5, 34.4, 30.5, 29.1, 27.1, 27.0, 25.1, 24.2, 24.1, 21.2. HRMS (ESI-TOF-MS): *m/z* calcd for $C_{146}H_{196}N_6O_{34}S_4$ $[M + 2H]^{2+}$ 1352.6338, found 1352.6331.

7NPD: 38.8 mg, 87%; ^{1}H NMR (600 MHz, CD_2Cl_2, 298 K): δ = 7.86–7.83 (m, 14H), 7.37–7.34 (m, 14H), 7.12 (s, 4H), 6.97 (s, 2H), 6.86–6.83 (m, 14H), 5.05 (s, 4H), 4.90 (s, 4H), 4.52 (t, *J* = 5.0 Hz, 4H), 4.27–4.24 (m, 28H), 3.97–3.95 (m, 28H), 3.87 (t, *J* = 5.0 Hz, 4H), 3.77–3.75 (m, 28H), 3.69–3.68 (m, 24H), 3.65–3.64 (m, 4H), 3.62 (br s, 8H), 3.59–3.54 (m, 2H), 3.44–3.39 (m, 4H), 3.19–3.15 (m, 2H), 3.12–3.08 (m, 2H), 2.47–2.42 (m, 2H), 2.38 (t, *J* = 5.0 Hz, 4H), 1.92–1.87 (m, 2H), 1.74–1.64 (m, 8H), 1.52–1.46 (m, 4H), 1.24 (d, *J* = 6.9 Hz, 24H) ppm. ^{13}C NMR (125 MHz, CD_2Cl_2, 298 K): δ = 173.6, 154.8, 153.3, 151.9, 144.5, 142.6, 136.2, 133.0, 128.7, 127.0, 125.8, 125.6, 124.7, 124.2, 114.7, 106.0, 71.0, 70.9, 70.1, 69.8, 68.5, 68.4, 68.2, 66.7, 56.8, 50.7, 40.6, 38.9, 35.0, 34.5, 34.4, 30.5, 29.1, 27.0, 26.0, 25.1, 24.2, 21.3 ppm. HRMS (ESI-TOF-MS): *m/z* calcd for $C_{182}H_{240}N_6O_{44}S_4$ $[M + 2H]^{2+}$ 1670.7799, found 1670.7838.

11NPD: 22.7 mg, 82%; ^{1}H NMR (600 MHz, CD_2Cl_2, 298 K): δ = 7.86–7.83 (m, 22H), 7.37–7.34 (m, 22H), 7.12 (s, 4H), 6.98 (s, 2H), 6.86–6.83 (m, 22H), 5.05 (s, 4H), 4.90 (s, 4H), 4.52 (t, *J* = 5.0 Hz, 4H), 4.27–4.24 (m, 44H), 3.96–3.94 (m, 44H), 3.87 (t, *J* = 5.0 Hz, 4H), 3.76–3.74 (m, 44H), 3.69–3.67 (m, 40H), 3.65–3.64 (m, 4H), 3.61 (br s, 8H), 3.59–3.54 (m, 2H), 3.44–3.39 (m, 4H), 3.19–3.15 (m, 2H), 3.12–3.08 (m, 2H), 2.47–2.41 (m, 2H), 2.39–2.33 (m, 4H), 1.92–1.87 (m, 2H), 1.73–1.62 (m, 8H), 1.50–1.45 (m, 4H), 1.24 (d, *J* = 6.9 Hz, 24H) ppm. ^{13}C NMR (125 MHz, CD_2Cl_2, 298 K): δ = 173.6, 154.7, 153.3, 151.8, 144.4, 142.6, 136.2, 133.0, 128.7, 127.0, 125.8, 125.6, 124.7, 124.2, 114.7, 106.0, 71.3, 71.0, 70.9, 70.1, 69.8, 68.5, 68.4, 68.2, 66.7, 56.8, 50.7, 40.6, 38.9, 35.0, 34.5, 34.4, 30.5, 30.1, 29.1, 27.0, 26.0, 25.1, 24.2, 21.2 ppm. HRMS (ESI-TOF-MS): *m/z* calcd for $C_{254}H_{328}N_6O_{64}S_4$ $[M + 2H]^{2+}$ 2307.0734, found 2307.0762.

15NPD: 22.1 mg, 79%; ^{1}H NMR (600 MHz, CD_2Cl_2, 298 K): δ = 7.85 (d, *J* = 8.5 Hz, 30H), 7.35 (t, *J* = 8.2 Hz, 30H), 7.12 (s, 4H), 6.98 (s, 2H), 6.86–6.83 (m, 30H), 5.05 (s, 4H), 4.90 (s, 4H), 4.52 (t, *J* = 5.0 Hz, 4H), 4.27–4.24 (m, 60H), 3.96–3.94 (m, 60H), 3.87 (t, *J* = 5.0 Hz, 4H), 3.76–3.74 (m, 60H), 3.69–3.67 (m, 56H), 3.65–3.64 (m, 4H), 3.61 (br s, 8H), 3.59–3.54 (m, 2H),

3.44–3.39 (m, 4H), 3.19–3.15 (m, 2H), 3.12–3.08 (m, 2H), 2.47–2.41 (m, 2H), 2.39–2.33 (m, 4H), 1.92–1.87 (m, 2H), 1.73–1.62 (m, 8H), 1.50–1.45 (m, 4H), 1.24 (d, J = 6.9 Hz, 24H) ppm. ^{13}C NMR (125 MHz, CD_2Cl_2, 298 K): δ = 173.5, 154.7, 153.3, 151.8, 144.4, 142.6, 136.2, 133.0, 128.7, 127.0, 125.8, 125.6, 124.7, 124.2, 114.7, 106.0, 71.3, 71.0, 70.9, 70.1, 69.8, 68.5, 68.4, 68.2, 66.7, 56.8, 50.7, 40.6, 38.9, 35.0, 34.5, 34.4, 30.5, 30.1, 29.1, 27.0, 26.5, 25.1, 24.2, 21.2 ppm. HRMS (ESI-TOF-MS): *m/z* calcd for $C_{326}H_{417}N_6O_{84}S_4$ $[M + 3H]^{3+}$ 1962.9152, found 1962.9192.

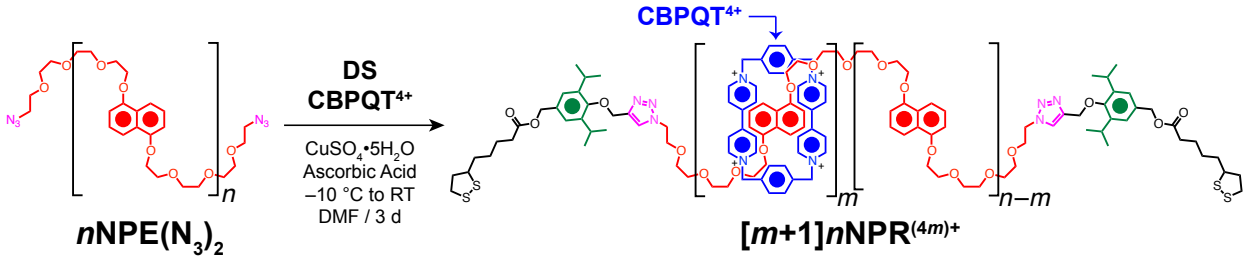

Scheme S6. Synthesis of donor-acceptor oligorotaxanes by the threading-followed-by-stoppering approach using click chemistry

General procedure for the synthesis of oligorotaxanes: The synthesis of rotaxane **[5]7NPR**·16PF_6 is given as a representative example. A mixture of **7NPE(N$_3$)$_2$** (124 mg, 0.05 mmol), **CBPQT**·4PF_6 (330 mg, 0.30 mmol), stopper **DS** (54.3 mg, 0.125 mmol), and ascorbic acid (35.2 mg, 0.2 mmol) in DMF (5 mL) was cooled to –10 °C. The deep red solution was stirred for 1 h, followed by addition of $CuSO_4$·5H_2O (25 mg, 0.1 mmol). The reaction mixture was stirred at –10 °C for 1 d and room temperature for an additional 2 d. The solvent was removed under vacuum to leave dark red gum, which was sequentially washed with CH_2Cl_2, aqueous EDTA solution, and H_2O. The residue was redissolved in MeCN:TFA (3:1 v/v, 40 mL) and stirred overnight. The solvent was evaporated and the residue was redissolved in Me_2SO (10 mL). The resulting dark red solution was filtered through a 0.2 μm PTFE filter, and subjected to chromatography by RP-HPLC with an eluant gradient of 0–60% in aqueous MeCN over 1 h at a flow rate of 20 mL·min^{-1}. The red-colored fractions were combined and subjected to repeated RP-HPLC purification using the same method. The purity of each fraction was checked by analytical HPLC before it was combined, concentrated, and precipitated in saturated aqueous NH_4PH_6 to afford a red precipitate, which was collected by filtration and washed with water, MeOH, ether, and dried under a flow of air.

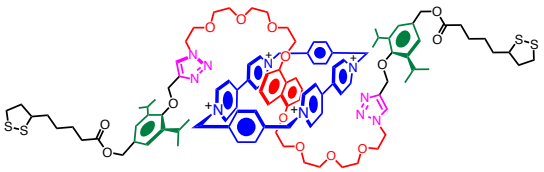

[2]1NPR^{4+}

[2]1NPR·4PF$_6$: (2× scale) 142 mg, 55%; ^{1}H NMR (600 MHz, CD_3CN, 233 K): δ = 8.96 (d, J = 6.6 Hz, 4H), 8.53 (d, J = 6.6 Hz, 4H), 7.95 (s, 4H), 7.93 (s, 2H), 7.80 (s, 4H), 7.35 (d, J = 6.6 Hz, 4H), 7.21 (s, 4H), 7.13 (d, J = 6.7 Hz, 4H), 6.15 (d, J = 7.8 Hz, 2H), 5.86 (t, J = 7.9 Hz, 2H), 5.63 (d, J = 13.6 Hz, 4H), 5.54 (d, J = 13.6 Hz, 4H), 5.00 (s, 4H), 4.77 (s, 4H), 4.20 (br s, 4H), 4.17 (br s, 4H), 4.15 (br s, 4H), 3.98 (br s, 4H), 3.79 (br s, 4H), 3.69 (br s, 4H), 3.56 (m, 2H), 3.50 (br s, 4H), 3.44 (hept, J = 6.9 Hz, 4H), 3.35 (br s, 4H), 3.16 (dt, J = 6.0, 12.0 Hz, 2H), 3.07 (dt, J = 7.0, 11.1 Hz, 2H), 2.44–2.39 (m, 2H), 2.35 (t, J = 7.3 Hz, 4H), 2.23 (d, J = 8.1 Hz, 2H), 1.87–1.81 (m, 4H), 1.72–1.65 (m, 2H), 1.62–1.51 (m, 6H), 1.43–1.33 (m, 4H), 1.19 (d, J = 6.8 Hz, 24H) ppm. ^{13}C NMR (125 MHz, CD_3CN, 298 K): δ = 174.1, 153.5, 52.0, 146.1, 144.4, 143.1, 137.5, 134.2, 132.3, 129.0, 125.3, 109.2, 105.1, 71.0, 70.7, 70.5, 69.6, 69.3, 68.5, 66.7, 66.0, 57.3, 50.6, 41.0, 39.2, 35.3, 34.6, 29.4, 25.5, 24.3 ppm. HRMS (ESI-TOF-MS): *m/z* calcd for $C_{110}H_{138}F_{18}N_{10}O_{14}P_3S_4$ $[M - PF_6]^+$ 2386.823, found 2386.819; *m/z* calcd for $C_{110}H_{138}F_{12}N_{10}O_{14}P_2S_4$ $[M - 2PF_6]^{2+}$ 1120.929, found 1120.931; *m/z* calcd for $C_{110}H_{138}F_6N_{10}O_{14}P_1S_4$ $[M - 3PF_6]^{3+}$ 698.964, found 698.966.

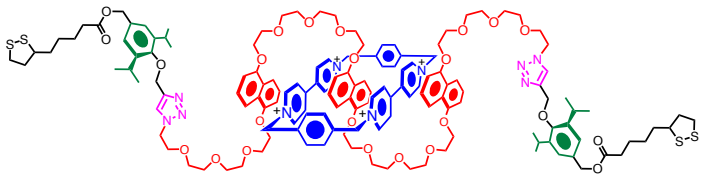

[2]3NPR^{4+}

[2]3NPR·4PF$_6$: 41 mg, 44%; ^{1}H NMR (600 MHz, CD_3CN, 233 K): δ = 8.73 (br s, 4H), 8.11 (d, J = 6.5 Hz, 4H), 8.03 (s, 2H), 7.82 (s, 4H), 7.73 (s, 4H), 7.18 (d, J = 7.8 Hz, 4H), 7.17 (s, 4H), 7.03 (t, J = 7.8 Hz, 4H), 6.54 (d, J = 6.0 Hz, 4H), 6.52 (d, J = 7.8 Hz, 4H), 6.45 (d, J = 6.0 Hz, 4H), 5.84 (d, J = 7.8 Hz, 2H), 5.70 (d, J = 13.7 Hz, 4H), 5.58 (t, J = 7.8 Hz, 2H), 5.52 (d, J = 13.8 Hz, 4H), 4.97 (s, 4H), 4.78 (s, 4H), 4.53 (t, J = 5.0 Hz, 4H), 3.99 (br s, 16 H), 3.88 (br s, 4H), 3.80 (br s, 12H), 3.66 (br s, 4H), 3.64 (br s, 4H), 3.57 (br s, 4H), 3.53 (br s, 4H), 3.50 (br s, 4H), 3.47 (br s, 4H), 3.42–3.37 (m, 6H), 3.29 (hept, J = 6.8 Hz, 4H), 3.15 (dt, J = 6.5, 12.5 Hz, 2H), 3.06 (dt, J = 6.9, 10.8 Hz, 2H), 2.43–2.38 (m, 2H), 2.33 (t, J = 7.4 Hz, 4H), 1.90 (d, J = 8.0

Hz, 2H), 1.86–1.79 (m, 2H), 1.70–1.62 (m, 2H), 1.60–1.49 (m, 6H), 1.41–1.30 (m, 4H), 1.16 (d, J = 6.8 Hz, 24H) ppm. ^{13}C NMR (125 MHz, CD_3CN, 298 K): δ = 174.0, 154.6, 153.6, 153.3, 151.7, 143.1, 143.0, 137.4, 134.2, 128.9, 126.6, 126.4, 125.7, 125.2, 125.1, 114.8, 108.8, 106.9, 106.7, 104.7, 80.0, 76.7, 71.6, 71.2, 71.0, 70.9, 70.7, 70.6, 70.2, 69.8, 68.8, 68.6, 66.7, 66.6, 65.8, 62.7, 57.2, 50.9, 41.0, 39.2, 35.2, 34.5, 30.3, 29.3, 27.5, 27.4, 25.4, 24.2, 24.1 ppm. HRMS (ESI-TOF-MS): *m/z* calcd for $C_{146}H_{182}F_{12}N_{10}O_{24}P_2S_4$ $[M - 2PF_6]^{2+}$ 1439.076, found 1439.074; *m/z* calcd for $C_{146}H_{182}F_6N_{10}O_{24}PS_4$ $[M - 3PF_6]^{3+}$ 911.062, found 911.064; *m/z* calcd for $C_{146}H_{182}N_{10}O_{24}S_4$ $[M - 4PF_6]^{4+}$ 647.306, found 647.306.

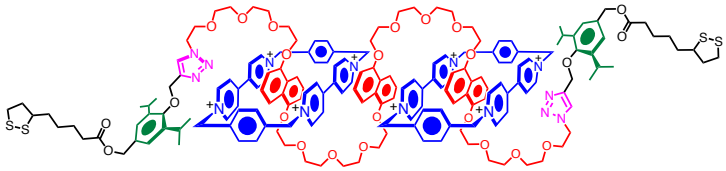

[3]3NPR^{8+}

[3]3NPR·8PF$_6$: 21 mg, 8%; ^{1}H NMR (600 MHz, CD_3CN, 233 K): δ = 8.88 (d, J = 6.5 Hz, 4H), 8.75 (d, J = 6.5 Hz, 4H), 8.39 (d, J = 6.6 Hz, 4H), 8.27 (d, J = 6.5 Hz, 4H), 7.91 (s, 2H), 7.87 (s, 4H), 7.85 (s, 4H), 7.73 (s, 4H), 7.71 (s, 4H), 7.19 (s, 4H), 6.98 (d, J = 6.0 Hz, 4H), 6.94 (d, J = 6.8 Hz, 8H), 6.86 (t, J = 7.8 Hz, 2H), 6.80–6.77 (m, 6H), 6.22 (d, J = 7.5 Hz, 2H), 6.03 (d, J = 7.8 Hz, 2H), 5.98 (d, J = 7.8 Hz, 2H), 5.75 (t, J = 7.8 Hz, 2H), 5.68 (t, J = 7.8 Hz, 2H), 5.64 (d, J = 13.5 Hz, 4H), 5.53 (d, J = 13.5 Hz, 4H), 5.52 (d, J = 13.5 Hz, 4H), 5.43 (d, J = 13.5 Hz, 4H), 4.99 (s, 4H), 4.75 (s, 4H), 4.16 (br s, 4H), 4.09 (br s, 8H), 4.06 (br s, 4H), 3.96 (br s, 4H), 3.92 (br s, 4H), 3.86 (br s, 4H), 3.77 (br s, 4H), 3.76 (br s, 4H), 3.66 (br s, 8H), 3.61 (br s, 4H), 3.56 (dt, J = 5.8, 11.7 Hz, 2H), 3.49 (br s, 8H), 3.43–3.37 (m, 8H), 3.16 (dt, J = 6.0, 11.8 Hz, 2H), 3.07 (dt, J = 7.0, 11.1 Hz, 2H), 2.45–2.33 (m, 2H), 2.32 (t, J = 7.4 Hz, 4H), 2.09 (d, J = 8.0 Hz, 2H), 2.02 (d, J = 8.0 Hz, 2H), 1.87–1.81 (m, 2H), 1.71–1.65 (m, 2H), 1.62–1.51 (m, 6H), 1.42–1.33 (m, 4H), 1.18 (d, J = 6.9 Hz, 24H) ppm. ^{13}C NMR (125 MHz, CD_3CN, 298 K): δ = 174.1, 153.6, 151.9, 145.6, 145.5, 145.4, 145.3, 145.2, 145.1, 144.6, 143.1, 137.4, 134.1, 132.1, 129.0, 126.7, 125.3, 125.2, 114.7, 109.0, 109.0, 106.8, 106.7, 105.1, 104.9, 72.1, 71.9, 71.6, 71.5, 71.4, 71.1, 71.0, 70.6, 70.5, 70.2, 69.6, 69.2, 68.8, 68.6, 66.7, 65.9, 57.3, 50.6, 41.1, 39.2, 35.3, 34.6, 29.4, 27.4, 25.5, 24.3 ppm. HRMS (ESI-TOF-MS): *m/z* calcd for $C_{182}H_{214}F_{36}N_{14}O_{24}P_6S_4$ $[M - 2PF_6]^{2+}$ 1989.637, found 1989.640; *m/z* calcd for $C_{182}H_{214}F_{30}N_{14}O_{24}P_5S_4$ $[M - 3PF_6]^{3+}$ 1278.103, found 1278.104.

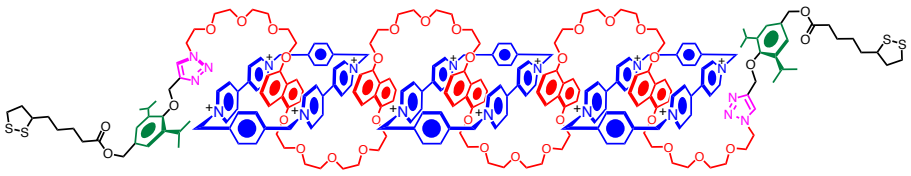

[4]5NPR^{12+}

[4]5NPR·12PF$_6$: 66 mg, 25%; ^{1}H NMR (600 MHz, CD_3CN, 233 K): δ = 8.84 (d, J = 6.4 Hz, 4H), 8.72 (d, J = 6.3 Hz, 4H), 8.62 (d, J = 6.5 Hz, 4H), 8.34 (d, J = 6.5 Hz, 4H), 8.24 (d, J = 6.5 Hz, 4H), 8.02 (d, J = 6.5 Hz, 4H), 7.90 (s, 2H), 7.83 (s, 8 H), 7.76 (s, 4H), 7.70 (s, 8H), 7.63 (s, 4 H), 7.19 (s, 4H), 6.93 (d, J = 6.0 Hz, 4H), 6.91 (d, J = 6.0 Hz, 8H), 6.80 (m, J = 7.8 Hz, 2H), 6.78 (t, J = 7.8 Hz, 2H), 6.75 (d, J = 6.0 Hz, 4H), 6.68 (d, J = 8.2 Hz, 2H) 6.64 (d, J = 8.2 Hz, 2 H), 6.50 (d, J = 6.4 Hz, 4H), 6.44 (d, J = 6.4 Hz, 4H), 6.12 (d, J = 7.6 Hz, 4H), 6.00 (d, J = 7.7 Hz, 2H), 5.96 (d, J = 7.7 Hz, 2H), 5.81 (d, J = 7.6 Hz, 2H), 5.72 (t, J = 7.7, 2H), 5.66 (t, J = 7.7 Hz, 2H), 5.61 (d, J = 14.0 Hz, 4H), 5.52 (t, J = 7.3 Hz, 2H) 5.49 (d, J = 14.0 Hz, 12H) 5.42–5.37 (m, 8H), 4.99 (s, 4H), 4.74 (s, 4H), 4.15 (br s, 8H), 4.07 (br s, 8H), 4.04 (br s, 4H), 3.96 (br s, 8H), 3.91 (br s, 8H), 3.85 (br s, 4H), 3.83 (br s, 4H), 3.75 (br s, 12H), 3.65 (br s, 8H), 3.62 (br s, 8H), 3.59–3.53 (m, 10H), 3.47 (br s, 8H), 3.46–3.36 (m, 12H), 3.16 (dt, J = 6.1, 11.8 Hz, 2H), 3.07 (dt, J = 6.9, 10.9 Hz, 2H), 2.44–2.38 (m, 2H), 2.34 (t, J = 7.5 Hz, 4H), 2.06 (d, J = 7.9 Hz, 2H), 1.99 (d, J = 7.9 Hz, 2H), 1.87–1.81 (m, 2H), 1.83 (d, J = 6.9 Hz, 2H), 1.72–1.65 (m, 2H), 1.61–1.52 (m, 6H), 1.42–1.34 (m, 4H), 1.88 (d, J = 6.6 Hz, 24H) ppm. ^{13}C NMR (125 MHz, CD_3CN, 298 K): δ = 172.8, 153.0, 152.3, 150.6, 144.2, 143.6, 143.2, 141.8, 136.0, 132.8, 130.8, 127.6, 125.4, 125.0, 124.0, 123.9, 113.4, 107.8, 105.5, 103.7, 103.6, 70.6, 70.2, 70.1, 69.7, 69.3, 69.2, 68.9, 68.3, 67.8, 67.4, 67.3, 65.4, 64.6, 56.0, 49.2, 39.7, 37.9, 33.9, 33.2, 29.6, 28.0, 26.1, 24.2, 23.0 ppm. HRMS (ESI-TOF-MS): *m/z* calcd for $C_{254}H_{290}F_{48}N_{18}O_{34}P_8S_4$ $[M - 4PF_6]^{4+}$ 1356.690, found 1356.686; *m/z* calcd for $C_{254}H_{290}F_{42}N_{18}O_{34}P_7S_4$ $[M - 5PF_6]^{5+}$ 1056.359, found 1056.362.

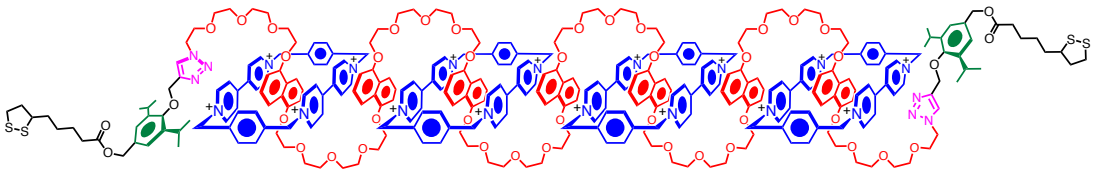

[5]7NPR^{16+}

[5]7NPR·16PF$_6$: 160 mg, 28%; ^{1}H NMR (600 MHz, CD_3CN, 233 K): δ = 8.84 (d, J = 6.4 Hz, 4H), 8.71 (d, J = 6.2 Hz, 4H), 8.60 (m, 8H), 8.33 (d, J = 6.6 Hz, 4H), 8.24 (d, J = 6.3 Hz, 4H),

8.02 (m, 8H), 7.89 (s, 2H), 7.83 (s, 8H), 7.74 (s, 8H), 7.69 (s, 8H), 7.62 (s, 8H), 7.18 (s, 4H), 6.90 (d, J = 6.5 Hz, 4H), 6.93 (d, J = 6.5 Hz, 8H), 6.78 (d, J = 8.0 Hz, 4H), 6.74 (d, J = 6.4 Hz, 4H), 6.72 (t, J = 7.5 Hz, 2H), 6.67 (d, J = 8.0 Hz, 2H), 6.63 (d, J = 8.0 Hz, 2H), 6.56 (d, J = 7.6 Hz, 2H), 6.49–6.46 (m, 8H), 6.43–6.40 (m, 8H), 6.12 (d, J = 7.7 Hz, 4H), 6.05 (d, J = 7.5 Hz, 2H), 6.00 (d, J = 7.5 Hz, 2H), 5.95 (d, J = 7.5 Hz, 2H), 5.79, (d, J = 7.5 Hz, 4H), 5.71 (t, J = 7.7 Hz, 2H), 5.65 (t, J = 7.7 Hz, 2H), 5.60 (d, J = 13.8, 4H), 5.52–5.34 (m, 32H), 4.98 (s, 4H), 4.74 (s, 4H), 4.15 (br s, 4H), 4.06 (br s, 16H), 3.95 (br s, 24H), 3.90 (br s, 12H), 3.85 (br s, 4H), 3.82 (br s, 8H), 3.75 (br s, 16H), 3.64 (br s, 8H), 3.61 (br s, 12H), 3.59–3.53 (m, 10H), 3.47 (br s, 4H), 3.44–3.36 (m, 16H), 3.16 (dt, J = 6.0, 12.0 Hz, 2H), 3.07 (dt, J = 7.0, 11.1 Hz, 2H), 2.44–2.38 (m, 2H), 2.34 (t, J = 7.4 Hz, 4H), 2.05 (d, J = 8.0 Hz, 2H), 1.99 (d, J = 8.0 Hz, 2H), 1.87–1.81 (m, 4H), 1.81 (d, J = 8.0 Hz, 4H), 1.71–1.64 (m, 2H), 1.62–1.51 (m, 4H), 1.42–1.32 (m, 4H), 1.17 (d, J = 6.8 Hz, 24H) ppm. ^{13}C NMR (125 MHz, CD_3CN, 298 K): δ = 172.8, 153.0, 152.3, 150.6, 144.2, 143.6, 143.2, 141.8, 136.0, 132.8, 130.8, 127.6, 125.4, 124.9, 124.4, 123.9, 113.4, 107.7, 105.5, 103.6, 70.6, 70.2, 70.1, 69.7, 69.3, 69.2, 68.9, 68.3, 67.8, 67.7, 67.4, 67.3, 65.4, 64.6, 64.5, 56.0, 49.2, 39.7, 37.9, 33.9, 33.2, 28.0, 26.1, 24.2, 23.0 ppm; HRMS (ESI-TOF-MS): *m/z* calcd for $C_{326}H_{366}F_{72}N_{22}O_{44}P_{12}S_4$ $[M - 4PF_6]^{4+}$: 1791.044, found: 1791.045; *m/z* calcd for $C_{326}H_{366}F_{66}N_{22}O_{44}P_{11}S_4$ $[M - 5PF_6]^{5+}$: 1403.842, found: 1403.840; *m/z* calcd for $C_{326}H_{366}F_{60}N_{22}O_{44}P_{10}S_4$ $[M - 6PF_6]^{6+}$: 1145.708; found: 1145.709.

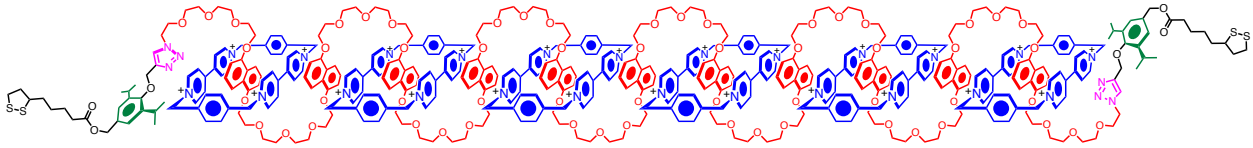

[7]11NPR^{24+}

[7]11NPR·24PF$_6$: 52 mg, 15%; ^{1}H NMR (600 MHz, CD_3CN, 233 K): δ = 8.84 (d, J = 6.0 Hz, 4H), 8.71 (d, J = 6.0 Hz, 4H), 8.62–8.58 (m, 8H), 8.58–8.53 (m, 8H), 8.33 (d, J = 6.5 Hz, 4H), 8.24 (d, J = 6.5 Hz, 4H), 8.02–7.98 (m, 8H), 7.98–7.95 (m, 8H), 7.89 (s, 2H), 7.83 (s, 8H), 7.74 (s, 8H), 7.72 (s, 8H), 7.69 (s, 8H), 7.61 (s, 8H), 7.60 (s, 8H), 7.18 (s, 4H), 6.93 (d, J = 6.0 Hz, 4H), 6.90 (d, J = 6.5 Hz, 8H), 6.78 (d, J = 8.0 Hz, 4H), 6.74 (d, J = 6.0 Hz, 4H), 6.73–6.68 (m, 6H), 6.67 (d, J = 8.0 Hz, 2H), 6.63 (d, J = 8.0 Hz, 2H), 6.56–6.51 (m, 6H), 6.49–6.46 (m, 8H), 6.45–6.42 (m, 8H), 6.42–6.39 (m, 8H), 6.39–6.35 (m, 8H), 6.11 (d, J = 7.3 Hz, 4H), 6.05–6.01 (m, 6H), 6.00 (d, J = 7.5 Hz, 2H), 5.95 (d, J = 7.5 Hz, 2H), 5.81–5.75 (m, 8H), 5.71 (t, J = 7.7

Hz, 2H), 5.66 (t, J = 7.7 Hz, 2H), 5.60 (d, J = 13.8 Hz, 4H), 5.50–5.31 (m, 60H), 4.98 (s, 4H), 4.73 (s, 4H), 4.15 (br s, 4H), 4.06 (br s, 16H), 3.95 (br s, 36H), 3.90 (br s, 24H), 3.84 (br s, 8H), 3.81 (br s, 16H), 3.75 (br s, 24H), 3.64 (br s, 8H), 3.61 (br s, 16H), 3.59–3.53 (m, 22H), 3.47 (br s, 4H), 3.43–3.31 (m, 20H), 3.16 (dt, J = 6.0, 12.0 Hz, 2H), 3.07 (dt, J = 7.0, 11.0 Hz, 2H), 2.46–2.36 (m, 2H), 2.34 (t, J = 7.4 Hz, 4H), 2.05 (d, J = 8.0 Hz, 2H), 1.99 (d, J = 8.0 Hz, 2H), 1.87–1.81 (m, 4H), 1.81–1.77 (m, 8H), 1.71–1.64 (m, 2H), 1.60–1.51 (m, 4H), 1.41–1.32 (m, 4H), 1.17 (d, J = 6.8 Hz, 24H) ppm. ^{13}C NMR (125 MHz, CD_3CN, 298 K): δ = 172.8, 153.0, 152.3, 150.6, 150.5, 144.2, 143.6, 143.2, 141.8, 136.1, 136.0, 132.8, 130.8, 127.7, 127.6, 125.4, 124.9, 124.6, 123.9, 113.4, 107.6, 105.5, 103.5, 70.6, 70.2, 70.1, 69.7, 69.3, 69.2, 68.9, 68.3, 67.8, 67.7, 67.4, 67.3, 65.4, 64.6, 64.5, 56.0, 49.2, 39.7, 37.9, 33.9, 33.2, 28.0, 26.1, 24.2, 23.0 ppm. HRMS (ESI-TOF-MS): *m/z* calcd for $C_{470}H_{518}F_{102}N_{30}O_{64}P_{17}S_4$ $[M - 7PF_6]^{7+}$: 1457.587, found: 1457.581; *m/z* calcd for $C_{470}H_{518}F_{96}N_{30}O_{64}P_{16}S_4$ calcd for $[M - 8PF_6]^{8+}$: 1257.268; found: 1257.268; *m/z* calcd for $C_{470}H_{518}F_{90}N_{30}O_{64}P_{15}S_4$ calcd for $[M - 9PF_6]^{9+}$: 1101.464; found: 1101.467.

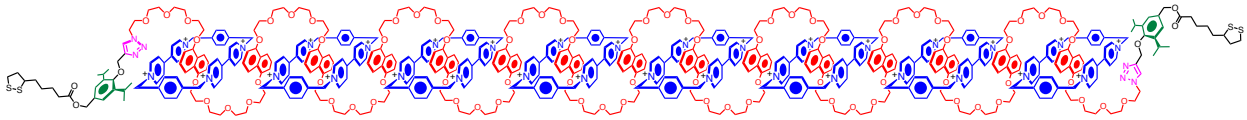

[9]15NPR^{32+}

[9]15NPR·32PF$_6$: 31 mg, 10%; ^{1}H NMR (600 MHz, CD_3CN, 233 K): δ = 8.84 (br s, 4H), 8.71 (br s, 4H), 8.59 (br s, 8H), 8.56 (br s, 16H), 8.33 (m, 8H), 8.23 (m, 8H), 8.00 (br s, 8H), 7.96 (br s, 8H), 7.89 (s, 2H), 7.83 (s, 8H), 7.74 (s, 8H), 7.72 (s, 16H), 7.69 (s, 8H), 7.60 (s, 8H), 7.59 (s, 16H), 7.18 (s, 4H), 6.93 (br s, 4H), 6.91 (br s, 8H), 6.78 (d, J = 8.0 Hz, 4H), 6.74 (br s, 4H), 6.73–6.67 (m, 12H), 6.64 (d, J = 7.7 Hz, 2H), 6.56–6.51 (m, 10H), 6.47 (br s, 12H), 6.42 (br s, 24H), 6.36 (br s, 12H), 6.12 (d, J = 7.5 Hz, 4H), 6.06–5.99 (m, 12H), 5.95 (d, J = 7.5 Hz, 2H), 5.82–5.73, (m, 12H), 5.71 (t, J = 7.7 Hz, 2H), 5.65 (t, J = 7.7 Hz, 2H), 5.63–5.29 (m, 76H), 4.98 (s, 4H), 4.73 (s, 4H), 4.14 (br s, 4H), 4.06 (br s, 16H), 3.95 (br s, 48H), 3.90 (br s, 36H), 3.84 (br s, 12H), 3.81 (br s, 24H), 3.75 (br s, 32H), 3.64 (br s, 8H), 3.61 (br s, 22H), 3.59–3.53 (m, 32H), 3.47–3.31 (m, 28H), 3.16 (dt, J = 6.0, 12.0 Hz, 2H), 3.07 (dt, J = 7.0, 11.0 Hz, 2H), 2.44–2.33 (m, 6H), 2.06 (d, J = 8.0 Hz, 2H), 1.99 (d, J = 8.0 Hz, 2H), 1.86–1.75 (m, 16H), 1.71–1.64 (m, 2H), 1.60–1.51 (m, 4H), 1.41–1.32 (m, 4H), 1.17 (d, J = 6.8 Hz, 24H) ppm. ^{13}C NMR (150 MHz, CD_3CN, 233 K): δ = 173.4, 152.7, 152.5, 152.3, 150.4, 144.2, 144.0, 143.4, 143.2, 143.0, 142.1,

136.4, 133.1, 131.1, 131.0, 130.7, 127.9, 125.8, 125.4, 124.7, 124.5, 123.9, 123.7, 123.0, 113.2, 107.2, 105.4, 103.4, 70.6, 70.3, 69.9, 69.7, 69.5, 69.0, 68.5, 67.8, 67.5, 67.4, 66.0, 64.6, 64.3, 56.4, 49.5, 40.2, 38.3, 34.5, 33.5, 28.7, 26.4, 24.5, 23.3 ppm. HRMS (ESI-TOF-MS): *m/z* calcd for $C_{614}H_{670}F_{126}N_{38}O_{84}P_{21}S_4$ $[M - 11PF_6]^{11+}$: 1190.735, found: 1190.730; *m/z* calcd for $C_{614}H_{670}F_{120}N_{38}O_{84}P_{20}S_4$ $[M - 12PF_6]^{12+}$: 1079.428, found: 1079.425.

3. Analysis of the ^{1}H NMR Spectra of the Oligorotaxanes

The ^{1}H NMR resonances of the oligorotaxanes were assigned with the aid of two-dimensional correlation spectroscopy and nuclear Overhauser effect (nOe) spectroscopy, namely ^{1}H–^{1}H gradient selected correlation spectroscopy (gCOSY) and ^{1}H–^{1}H gradient selected nuclear Overhauser effect spectroscopy (gNOESY). ^{1}H NMR spectra of **[2]1NPR^{4+}**, **[2]3NPR^{4+}**, **[3]3NPR^{8+}**, **[4]5NPR^{12+}**, **[5]7NPR^{16+}**, **[7]11NPR^{24+}**, and **[9]15NPR^{32+}** were acquired in CD_3CN at 233 K, where dynamic processes associated with pirouetting motions of 1,5-dioxynaphthalene (DNP) unit and CBPQT^{4+} rings with respect to each other and rotation of the bipyridinium (BIPY^{2+}) units through the cyclophane's cavity are 'frozen out' in a slow exchange regime on the NMR timescale. Note that only oligorotaxanes within the *Happy* series – those having 0.5(*n*–1)+2 components – express a single translational isomer, while the ^{1}H NMR signals of *Confused* and *Frustrated* oligorotaxanes are exceedingly difficult to assign by contrast, with the exception of **[2]3NPR^{4+}**, which has only two translational isomers. The ^{1}H NMR analyses for each of the oligorotaxanes we were capable of unraveling are discussed in detail below.

3A. ^{1}H NMR Spectroscopic Analysis of [2]1NPR·4PF$_6$

Assignment of the ^{1}H NMR spectrum (Figure S2) of **[2]1NPR^{4+}** is trivial in light of many previous studies on analogous compounds. This [2]rotaxane serves as an important model compound for comparing the effects of oligomerization on the chemical shifts of DNP and CBPQT^{4+} protons. **[2]1NPR^{4+}** has higher symmetry (see Figure 4 and the corresponding discussion in the main text) than the larger multicomponent oligomers because it possesses a single CBPQT^{4+} ring on a symmetrical dumbbell, leading to two α and two β signals from the BIPY^{2+} protons as a result of the C_2 symmetry of the DNP dumbbell being imposed on the CBPQT^{4+} ring. This separation of α and β signals verifies that DNP and BIPY^{2+} units do not undergo significant rearrangements (i.e. rotations that lead to signal averaging) on the timescale of the NMR experiment at 233 K in CD_3CN.

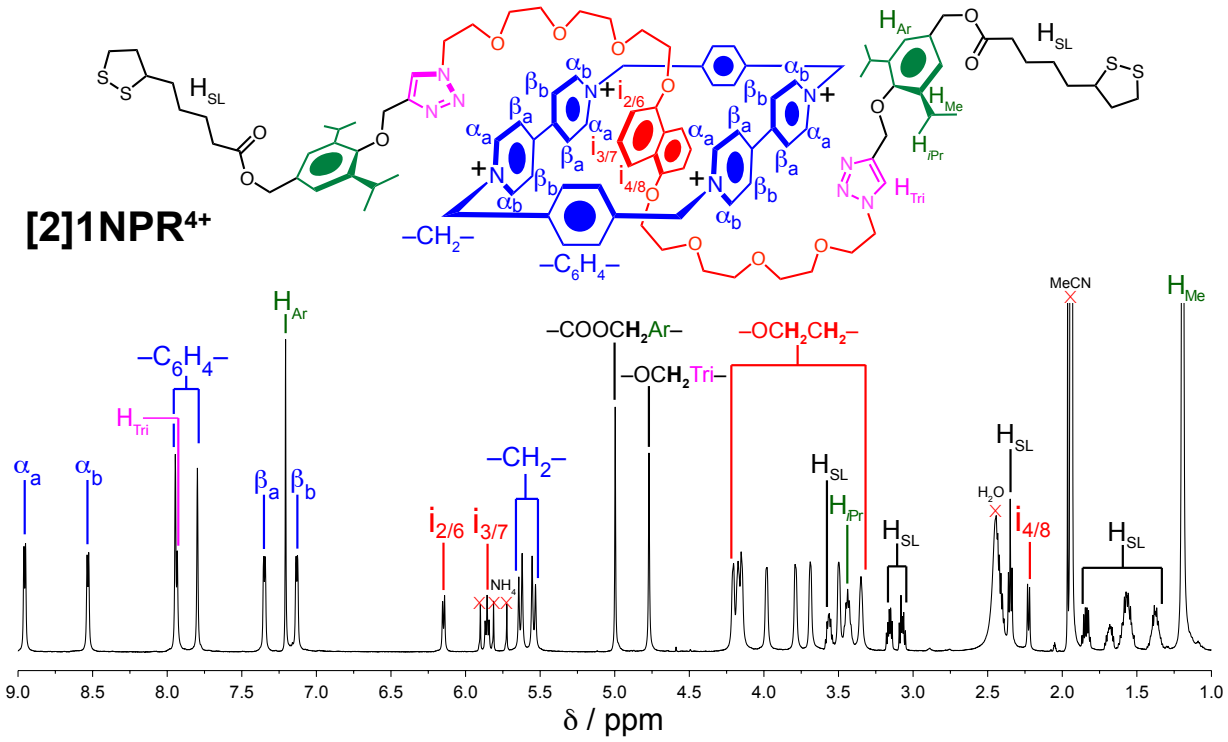

Figure S2. ^{1}H NMR spectrum (600 MHz) of **[2]1NPR**·4PF_6 in CD_3CN at 233 K

3B. ^{1}H NMR Spectroscopic Analysis of [2]3NPR·4PF_6

Although **[2]1NPR**$^{4+}$ represents a control compound for probing the effects of oligomerization on the chemical shifts of CBPQT^{4+} and included DNP protons, it has no alongside protons to serve as a basis for comparison. Therefore, **[2]3NPR**$^{4+}$ represents the best model for approximating the chemical shift of an 'alongside' DNP resonance in a two-component rotaxane. Unfortunately, **[2]3NPR**$^{4+}$ is not a *Happy* rotaxane; it belongs instead to the *Confused* series. Two translational isomers are allowed (Scheme S7) for this compound: one in which the CBPQT^{4+} ring encircles the central DNP unit, and one in which it occupies a DNP unit at the dumbbell terminus. These two isomers were found by integration of the ^{1}H NMR spectrum (Figure S3) to exist in a 4:1 ratio.

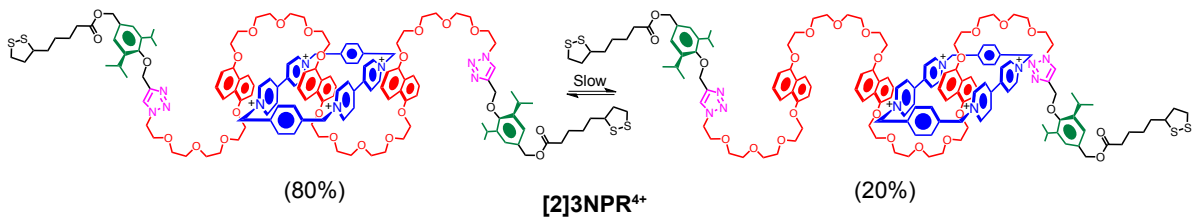

Scheme S7. Equilibrium between two translational isomers of **[2]3NPR**$^{4+}$ in CD_3CN at 233 K

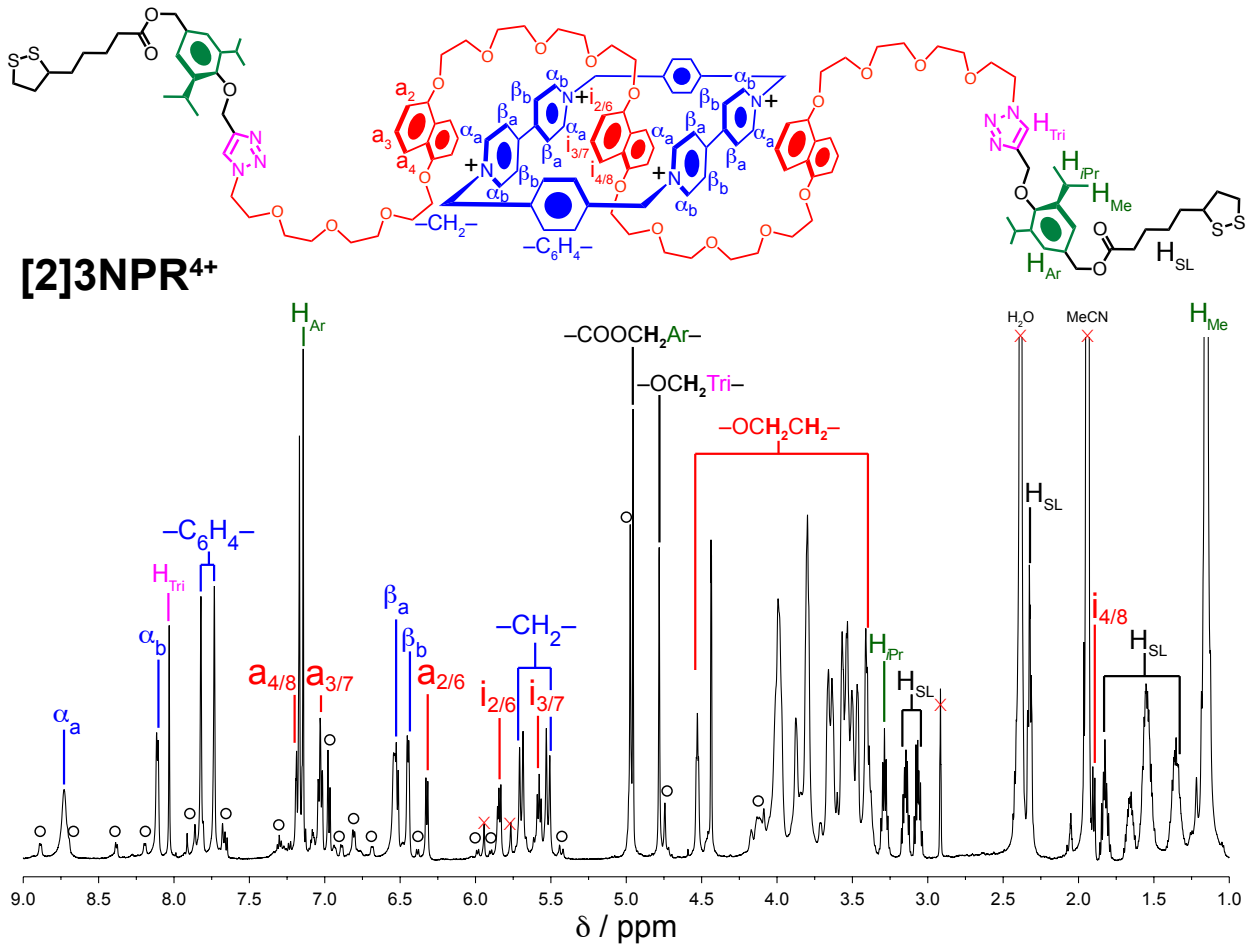

Figure S3. ^{1}H NMR spectrum (600 MHz) of **[2]3NPR**·4PF$_6$ in CD$_3$CN at 233 K

The unequal distribution of the two isomers can be accounted for on the basis that the translational isomer in which the CBPQT^{4+} ring occupies the central unit is more stabilized by an extended D-A stack, since it has twice as many alongside DNP–BIPY^{2+} interactions as there are in the terminal isomer. Signals are assigned to the major (80%) translational isomer in Figure S3, while those corresponding to the minor (20%) isomer are designated with open circles.

3C. ^{1}H NMR Spectroscopic Analysis of [3]3NPR·8PF$_6$

The first example of an oligomer in the *Happy* rotaxane series having more than one CBPQT^{4+} ring, namely **[3]3NPR^{8+}**, has reduced symmetry in comparison with the two-component systems featured in Sections 3A and 3B. The well-resolved signals with narrow linewidths in the ^{1}H NMR spectrum (Figure S4) clearly belong to a single isomer.

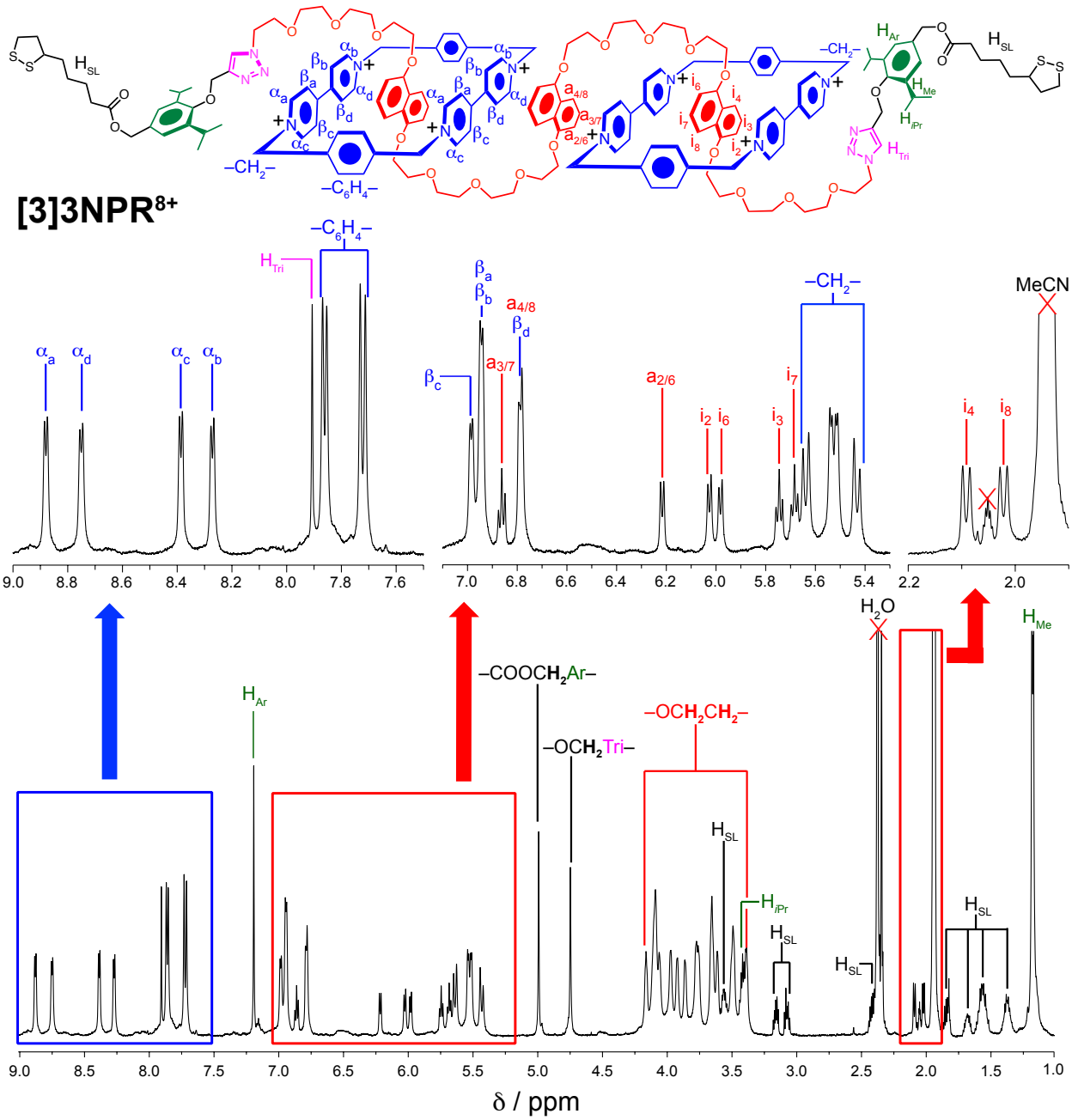

Figure S4. ^{1}H NMR spectrum (600 MHz) of **[3]3NPR**·8PF_6 in CD_3CN at 233 K

It is noted in the main text that the presence of only four α and four β signals means that the folded co-conformations represented by the structural formulas are not static on the NMR timescale, since the two (constitutionally equivalent) $CBPQT^{4+}$ rings would have eight heterotopic α sites and eight heterotopic β sites under conditions of slow co-conformational reorganization on the ^{1}H NMR timescale.

The signals could be assigned unambiguously by consulting the ^{1}H–^{1}H gCOSY and ^{1}H–^{1}H gNOESY spectra (Figures S5 and S6). A detailed discussion of how the signals were assigned for **[4]5NPR**$^{12+}$, which is presented in Section 3D, is also applicable to the ^{1}H NMR data for **[3]3NPR**·8PF_6, and so it will not be repeated here.

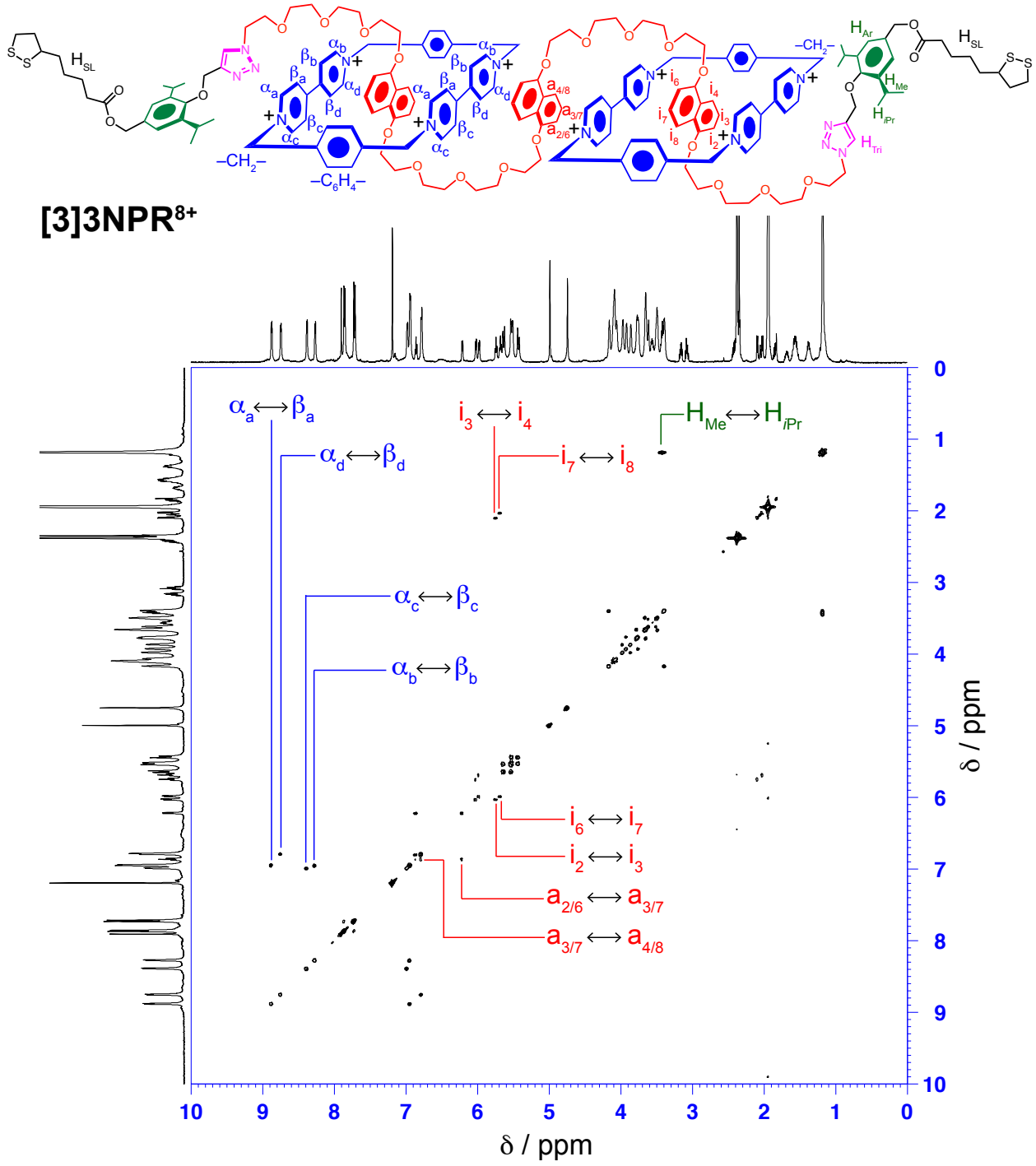

Figure S5. ^{1}H–^{1}H gCOSY spectrum (600 MHz) of **[3]3NPR**·8PF_6 in CD_3CN at 233 K

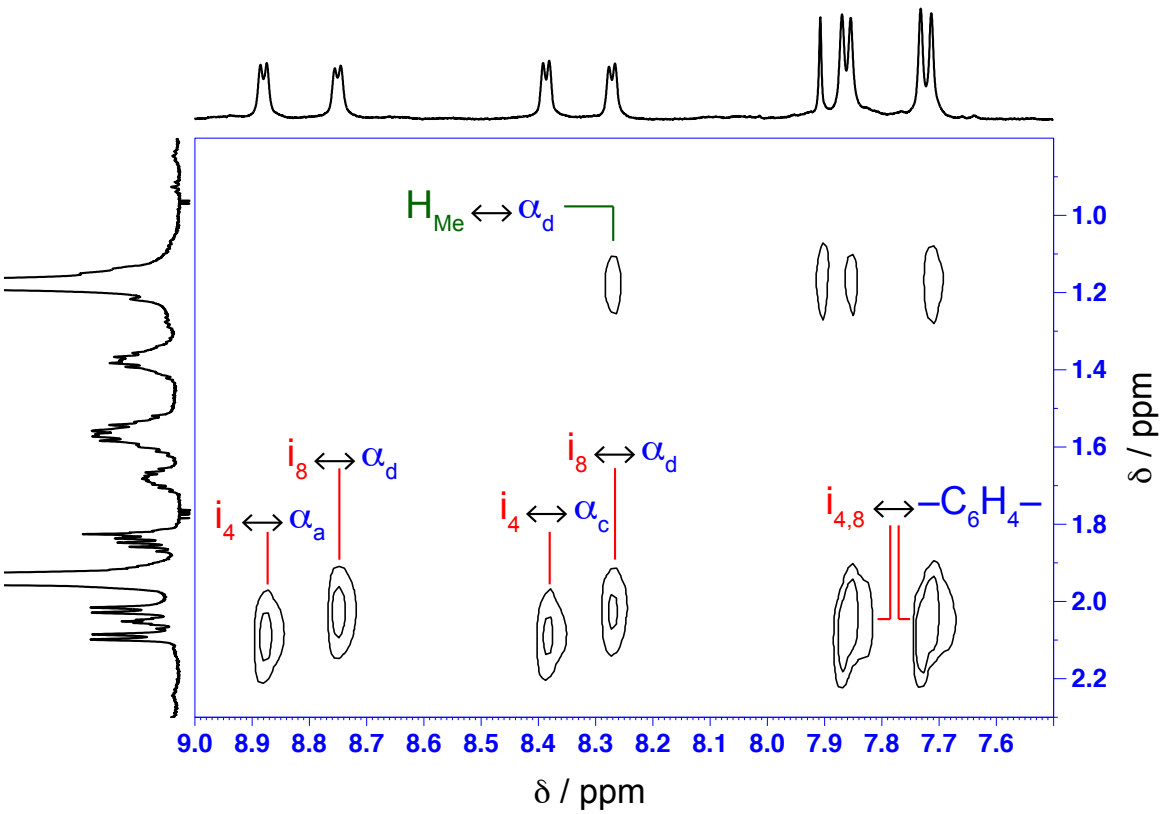

Figure S6. Partial ^{1}H–^{1}H gNOESY spectrum (600 MHz) of **[3]3NPR**·8PF$_6$ in CD$_3$CN at 233 K, showing the signals most relevant to structural assignments

3D. ^{1}H NMR Spectroscopic Analysis of [4]5NPR·12PF$_6$

In a previous analysis[S3] of a close analogue of **[4]5NPR**$^{12+}$ – differing only in the functionality at the 4–position of the aryl stopper – we assigned the ^{1}H NMR signals on the assumption of a folded secondary structure that was long-lived on the NMR timescale – i.e., slow exchange regime – leading us to distinguish between 'outside' (designated with the prefix 'o') and 'alongside' (designated with the prefix 'a') BIPY^{2+} units for the outer rings of the oligomer. In the folded co-conformation of **[4]5NPR**$^{12+}$, all eight α protons (and all eight β protons) of the outermost cyclophane are heterotopic because there are no local axes, planes, or centers of symmetry. Taking into account the inner ring, with its higher symmetry on account of an inversion center, there are a total of 12 α and 12 β heterotopic proton environments in the folded co-conformation of **[4]5NPR**$^{12+}$. Since only six α and six β resonances were observed in the ^{1}H NMR spectrum, it was implied in the previous analysis that certain pairs of α protons (and likewise pairs of β protons) resonated at the same frequency despite their heterotopicity.

An alternative and more realistic explanation for the observation of six instead of 12 sets of α and β resonances in the ^{1}H NMR spectrum of **[4]5NPR^{12+}** is that the [4]rotaxane interconverts (Scheme S8) between multiple folded (and, likely to a much lesser extent, unfolded) co-conformations quickly on the timescale of the NMR experiment. In this scenario, the ^{1}H signals represent an average of the resonances in each co-confomation as well as in their intermediate states, and therefore can be understood and interpreted with respect to the co-conformation of highest possible symmetry. Scheme S8 shows how the 'outside' and 'alongside' BIPY^{2+} units of the outer ring can be exchanged by executing a 180° rotation on the DNP⊂CBPQT^{4+} subcomplex. It transpires that additional data for the [4]rotaxane that were not included in our previous report[S3] – namely, ^{1}H–^{1}H gNOESY,– have revealed that this interpretation is the correct one on the basis of specific through-space correlations (*vide infra*) between DNP and BIPY^{2+} protons. In the case of **[4]5NPR^{12+}**, we retain the distinction between 'a' and 'o' resonances in order to remain consistent with our previous report and also to aid our description of the molecular dynamics in play. However, 'a' and 'o' resonances with the same subscript – e.g., oα_a and aα_a or oβ_d and aβ_d – are, in fact, undergoing fast exchange on the ^{1}H NMR timescale at 233 K in CD_3CN.

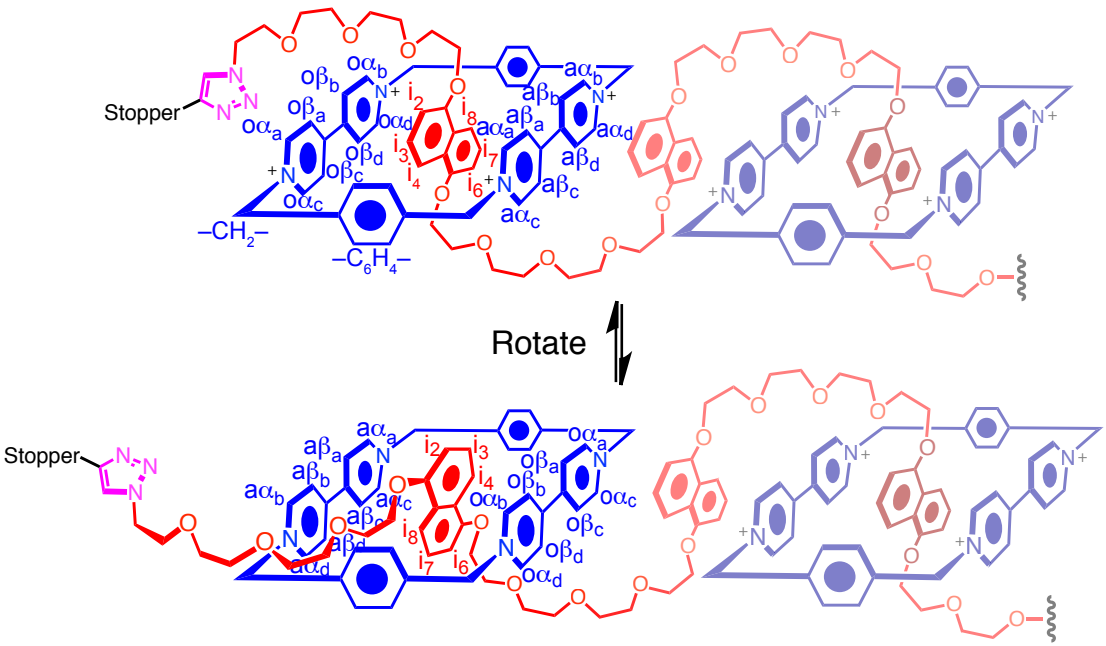

Scheme S8. The equilibration between two (of many) folded secondary structures of **[4]5NPR^{12+}**, showing how a 180° rotation of the outer DNP⊂CBPQT^{4+} complex causes 'outside' and 'alongside' BIPY^{2+} units to exchange positions in the D-A stack.

We turn our attention now to a detailed description of how the ^{1}H NMR signals were assigned (Figure S7) and how our conclusions about the solution-state structure were reached. Firstly, the higher symmetry of the central CBPQT^{4+} ring facilitated assignment of the resonances, since the two phenylene –C_6H_4– signals of the central ring can be assigned on the basis of integrated intensities alone, and the remaining resonances discerned through cross-peaks in the ^{1}H–^{1}H gCOSY (Figure S8) and ^{1}H–^{1}H gNOESY (Figures S9 and S10) spectra.

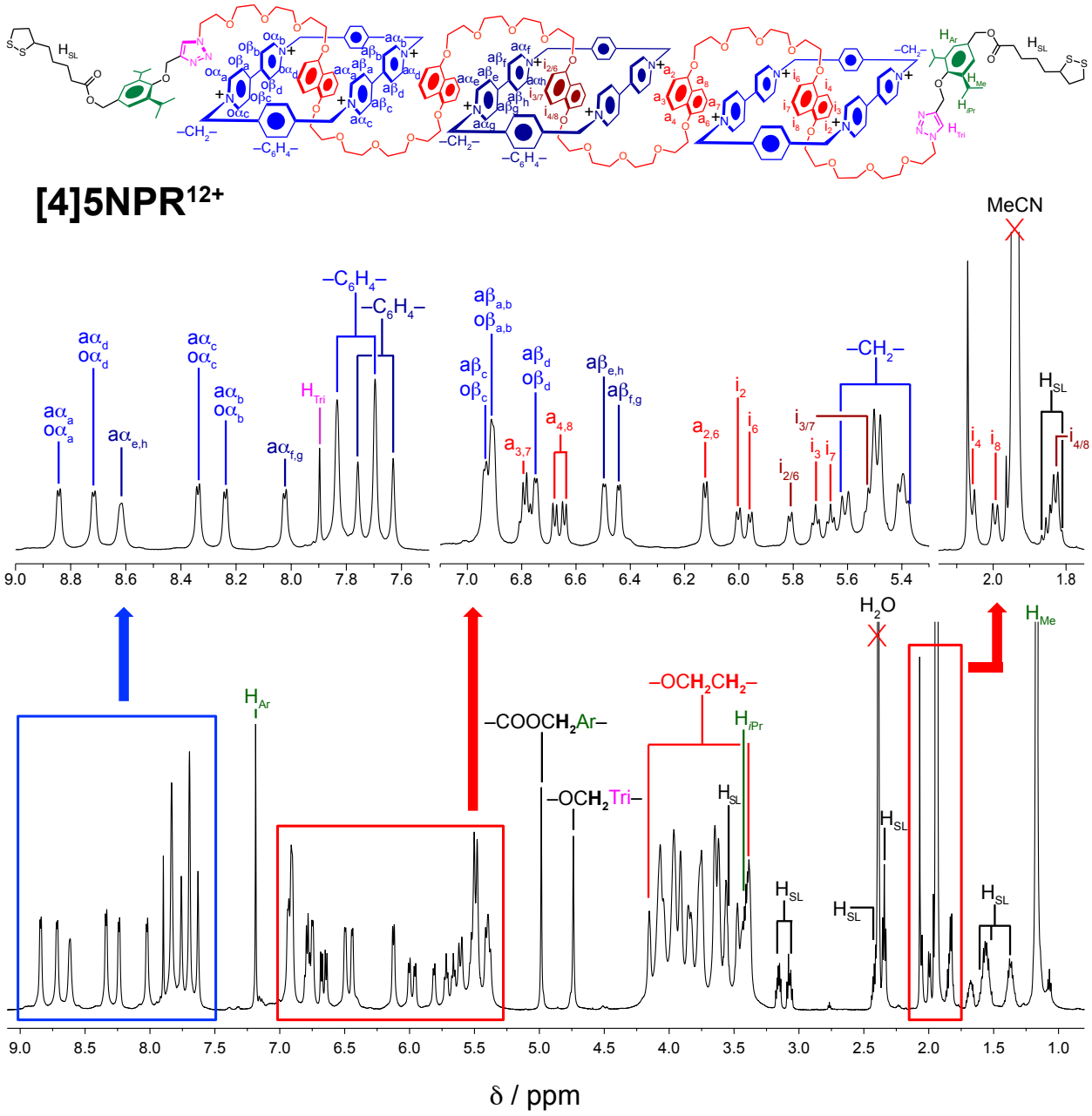

Figure S7. ^{1}H NMR spectrum (600 MHz) of **[4]5NPR**·12PF_6 in CD_3CN at 233 K

It is noteworthy that the α and β resonances for the innermost CBPQT^{4+} ring ($\alpha_{e–h}$ and $\beta_{e–h}$) are shifted to lower frequencies with respect to their counterparts in the outer rings and are also slightly broadened. Both of these features support the hypothesis of extended donor-acceptor π–π stacking in these rotaxanes, since alongside interactions from DNP units will shield the innermost ring and also slightly inhibit its (co)conformational freedom, leading to slower nuclear relaxation and line broadening.

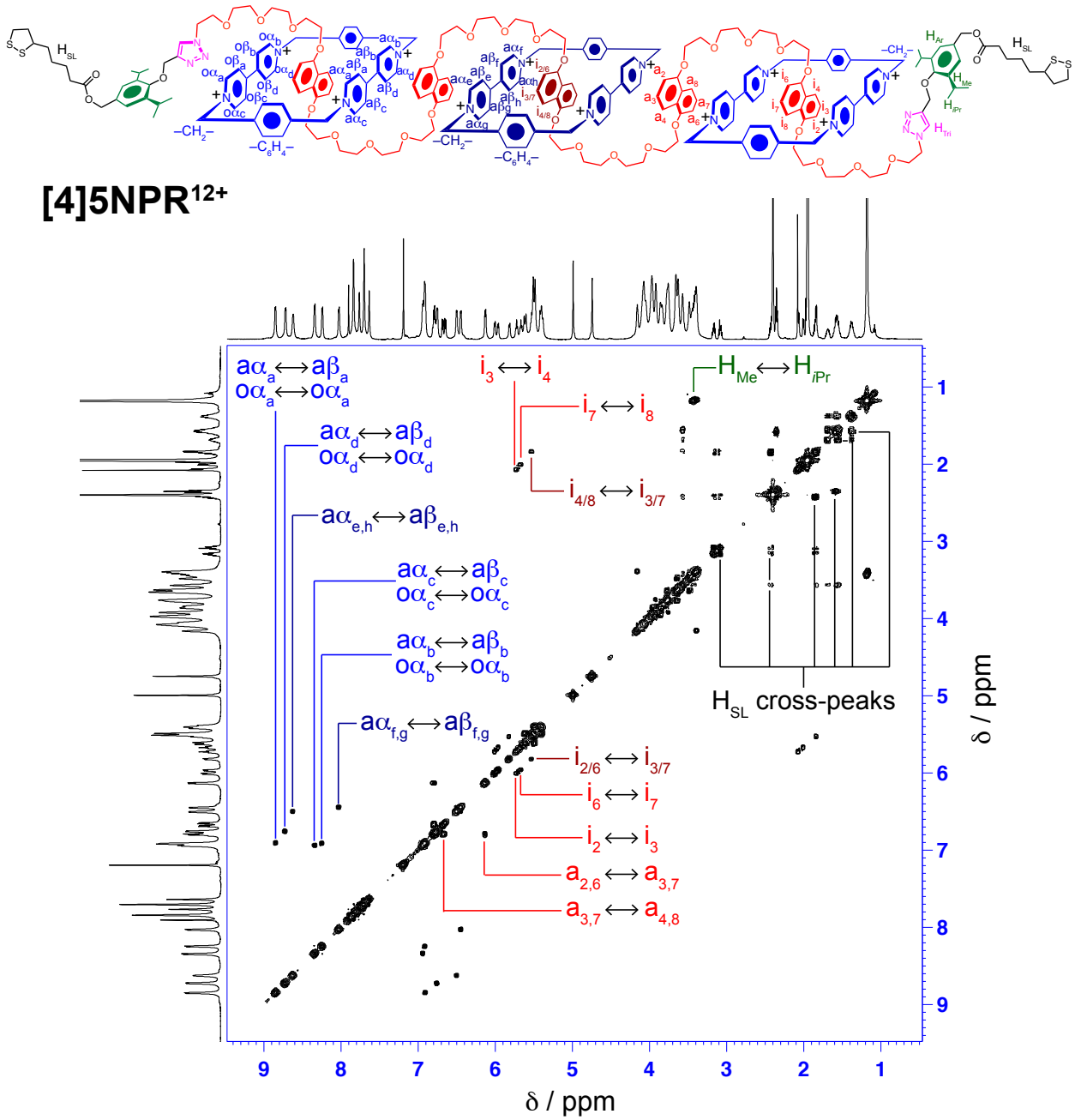

Figure S8. ^{1}H–^{1}H gCOSY spectrum (600 MHz) of **[4]5NPR**·12PF$_6$ in CD_3CN at 233 K

The ^{1}H–^{1}H gCOSY spectrum (Figure S8) reveals the coupling between each of the six α and β resonances of CBPQT^{4+}, as well as between neighboring protons in DNP subunits located inside (designated with a 'i') and alongside (designated with an 'a') the CBPQT^{4+} rings. In addition, the gCOSY spectrum revealed which signals correspond to the stoppers: the isopropyl resonance H_{iPr} could be identified among the –OCH$_2$CH$_2$O– resonances through its coupling with H_{Me}, and the set of multiplets belonging to the thioctic acid moiety could also be identified.

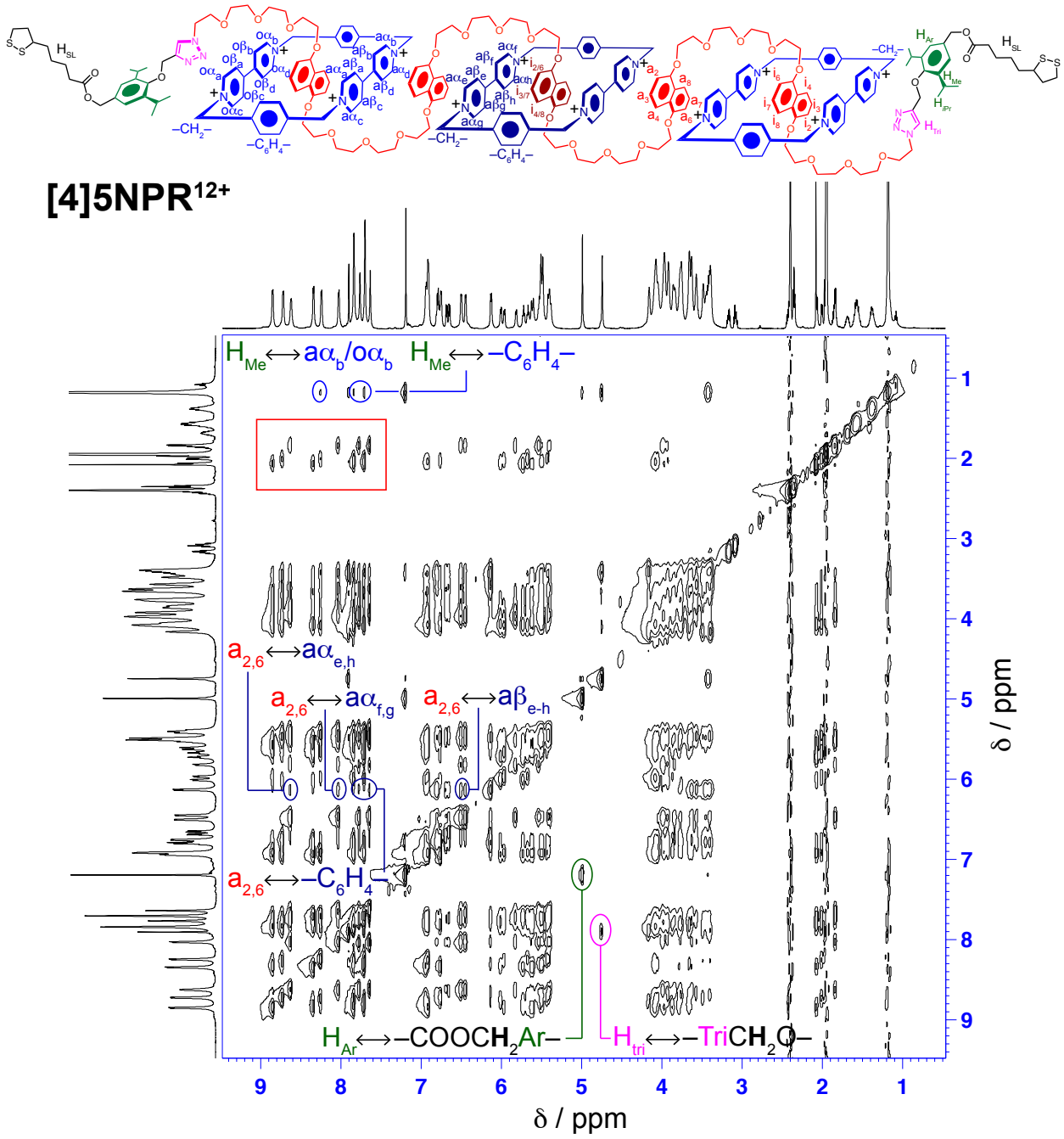

Figure S9. ^{1}H–^{1}H gNOESY spectrum (600 MHz) of **[4]5NPR**·12PF$_6$ in CD$_3$CN at 233 K

The ^{1}H–^{1}H gNOESY spectrum (Figure S9) was critical to both the full assignment of signals and to solution-state structural elucidation. For example, the assignment of the methylene signals associated with the stopper was confirmed by their through-space interactions with the aryl and triazole protons H_{Ar} and H_{Tri}, respectively. Particularly important are the nOe correlations between the 4/8 protons of 'inside' DNP units and the α and $–C_6H_4–$ resonances of $CBPQT^{4+}$. Since the three unique 'i' DNP proton environments at the 4– and 8–positions do not resonate at overlapping frequencies, their observed nOe correlations with the α $CBPQT^{4+}$ protons permit their unambiguous assignment. This section of the ^{1}H–^{1}H gNOESY spectrum is isolated in Figure S10.

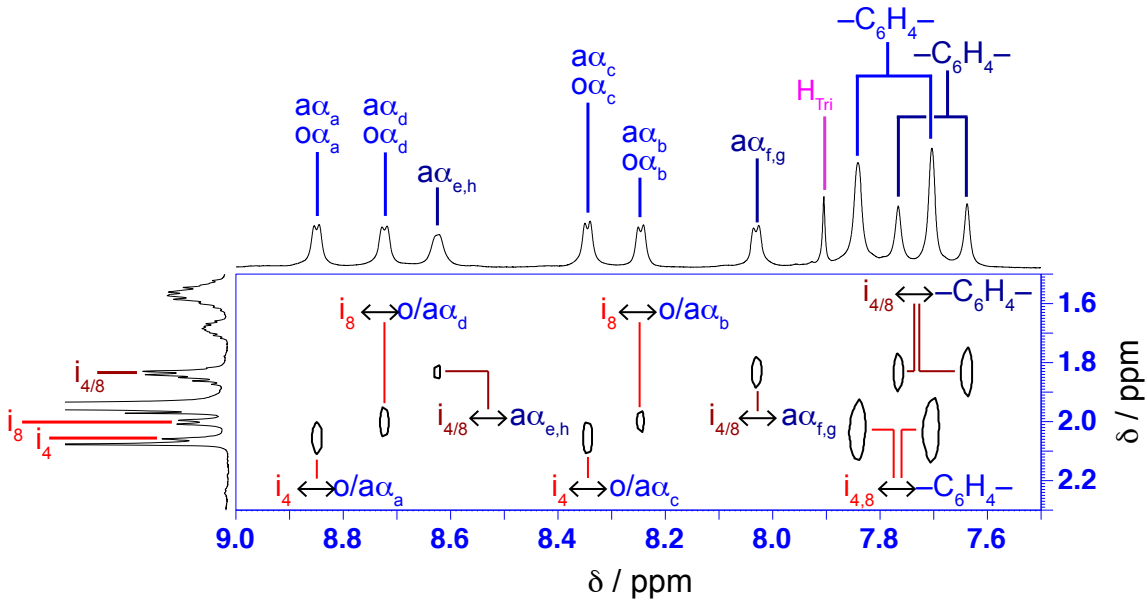

Figure S10. Partial ^{1}H–^{1}H gNOESY spectrum (600 MHz, CD_3CN, 233 K) showing correlations between DNP proton resonances corresponding to i_4, i_8, $i_{4/8}$ and the α and $–C_6H_4–$ ^{1}H signals of $CBPQT^{4+}$ in **[4]5NPR**·$12PF_6$ (boxed in red in Figure S9)

In order to underline the key insights provided by the 2D NOESY section in Figure S10, we turn our attention to the three highest-frequency resonances at 8.84 ppm, 8.72 ppm, and 8.62 ppm as demonstrative examples. Originally, we ascribed[S3] the 8.84 ppm resonance to $a\alpha_e$ and $a\alpha_h$, the 8.72 ppm resonance to $a\alpha_b$ and $a\alpha_c$, and the 8.62 ppm resonance to $o\alpha_a$ and $o\alpha_d$. In these assignments, the protons within each pair are located on opposite pyridinium rings of a single $BIPY^{2+}$ subunit. However, the three well-resolved DNP signals i_4, i_8, & $i_{4/8}$ in the region ca. 1.8–2.1 ppm each correlate through-space with exclusively *one* of the three α ^{1}H environments under

consideration. This fact is important because it leads us unequivocally to the conclusion that each signal corresponds, not to α protons located on the same $BIPY^{2+}$ subunit, but instead to α protons on opposite $BIPY^{2+}$ sites that are adjacent to the same phenylene ring of the cyclophane. The basis for this conclusion is the well known[S5] phenomenon – based primarily on dozens of crystal structures and dramatic changes in chemical shifts – in which each of the protons at the 4- and 8-positions of the DNP guest are directed by [C–H···π] interactions toward the center of a phenylene ($–C_6H_4–$) ring. From this location, no nOe correlation with two α protons on opposite poles of the $CBPQT^{4+}$ ring could be reasonably expected, and thus the nOe cross-peaks were assigned to $i_4 \leftrightarrow o/a\alpha_a$, $i_8 \leftrightarrow o/a\alpha_d$, and $i_{4/8} \leftrightarrow \alpha_{f,g}$. The nOe correlations are noted in a structural illustration for visualization purposes in Figure S11.

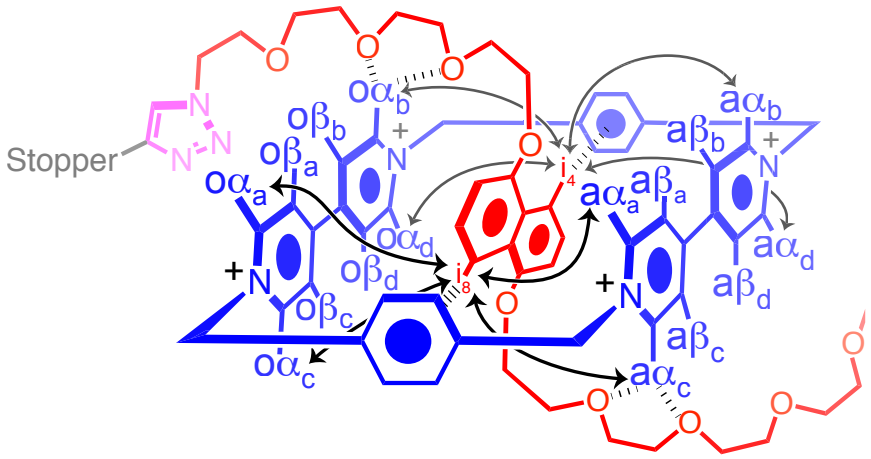

Figure S11. The nOe correlations observed between protons at the 4- and 8-positions of included DNP guests and the α protons of the $CBPQT^{4+}$ rings at the terminal sites of **[4]5NPR^{12+}**. Through-space correlations for i_4 and i_8 protons are each confined exclusively to one hemisphere of the cyclophane on account of noncovalent bonding interactions (dashed lines) that direct them toward the center of a phenylene group

The i_4 and i_8 proton signals were among the most challenging designations to define unambiguously. Our explicit assignments were made on the basis of several indirect arguments that were all consistent with the same conclusion. Firstly, we expected the i_8 protons, which are directed away from the stoppers toward the interior of the rotaxane, to resonate at slightly lower frequency than i_4 protons because they may be slightly more shielded in that local environment. We also encountered (Figure S9) a weak nOe signal between the H_{Me} stopper protons and α_b.

This nOe correlation was made more relevant by following the correlations from H_{Me}↔a/oα_b to a/oα_b↔i_4, since the [C–H···O] interactions between α protons and the electron-rich polyether chains (which are also observable in the crystal structure of many analogous compounds, see Ref. 17 in the main text) would likely place the stopper nearest in space to aα_b/oα_b. Furthermore, the proximity of α_b to the terminal polyether segment having the most conformational freedom is consistent with its chemical shift bearing the lowest frequency among all of the α protons of the terminal $CBPQT^{4+}$ rings. Although these arguments support our specific assignments of i_4 and i_8, we leave open the possibility that they may be transposed.

Having arrived at a description of the oligorotaxane as a rapidly exchanging foldamer in solution, we wish to point out that the dynamic nature of the folded state is not entirely surprising; with no strong bonds, either covalent or mechanical, that permanently fix two $BIPY^{2+}$ subunits on different $CBPQT^{4+}$ rings at a distance of ca. 0.7 Å – a distance that underpins the recognition properties of the $CBPQT^{4+}$ ring by allowing a planar entitiy to fit inside with nearly perfect π–π contacts – one would expect the association between unencircled 'alongside' DNP units and 'alongside' $BIPY^{2+}$ units to be many orders of magnitude weaker than those observed for $CBPQT^{4+}$ inclusion complexes, and therefore to be much more transient because of the correspondingly lower activation barriers. This is not to say that the folded co-conformation is absent in solution. Indeed, our claim that an extended donor-acceptor π-stack is a significant contributor to the solution-state structure of **[4]5NPR^{12+}** is supported, not only by the displaced chemical shifts of the alongside DNP protons and the innermost DNP⊂$CBPQT^{4+}$ resonances relative to both their uncomplexed dumbbell/cyclophane counterparts and even to their more peripherally-located cousins within the same rotaxane, but also by nOe correlations (Figure S9) between alongside DNP protons a_2, a_6, and the inner $CBPQT^{4+}$ resonances a$\alpha_{e–h}$. These correlations would be expected in a folded secondary structure in which the alongside DNP units interact with the $BIPY^{2+}$ units of the $CBPQT^{4+}$ ring.

3E. ^{1}H NMR Spectroscopic Analysis of [5]7NPR·16PF_6

In **[5]7NPR^{16+}** and larger oligorotaxanes, we forsake the extraneous designation between outer and alongside α and β $BIPY^{2+}$ environments since they undergo fast site exchange and drop the 'o' and 'a' prefixes. The presence of multiple inequivalent 'included' DNP sites also made it

necessary to further distinguish between 'i' DNP resonances. Therefore, included DNP units are iteratively designated with an additional 'i' moving toward the center of the rotaxane from the periphery. Thus, in **[5]7NPR**$^{16+}$, the innermost included DNP protons are designated 'ii', while the outermost included DNP protons retain the 'i' label. Although they are formally constitutionally heterotopic – in contrast with $i_{4/8}$ of **[4]5NPR**$^{12+}$ – the resonances of ii_4 & ii_8, ii_3 & ii_7, and ii_2 & ii_6 overlap, so their corresponding single signals are labeled $ii_{4,8}$, $ii_{3,7}$, and $ii_{2,6}$, respectively. As usual, the ^{1}H NMR signals were assigned (Figure S12) with the aid of multidimensional ^{1}H–^{1}H correlation and nOe spectroscopies.

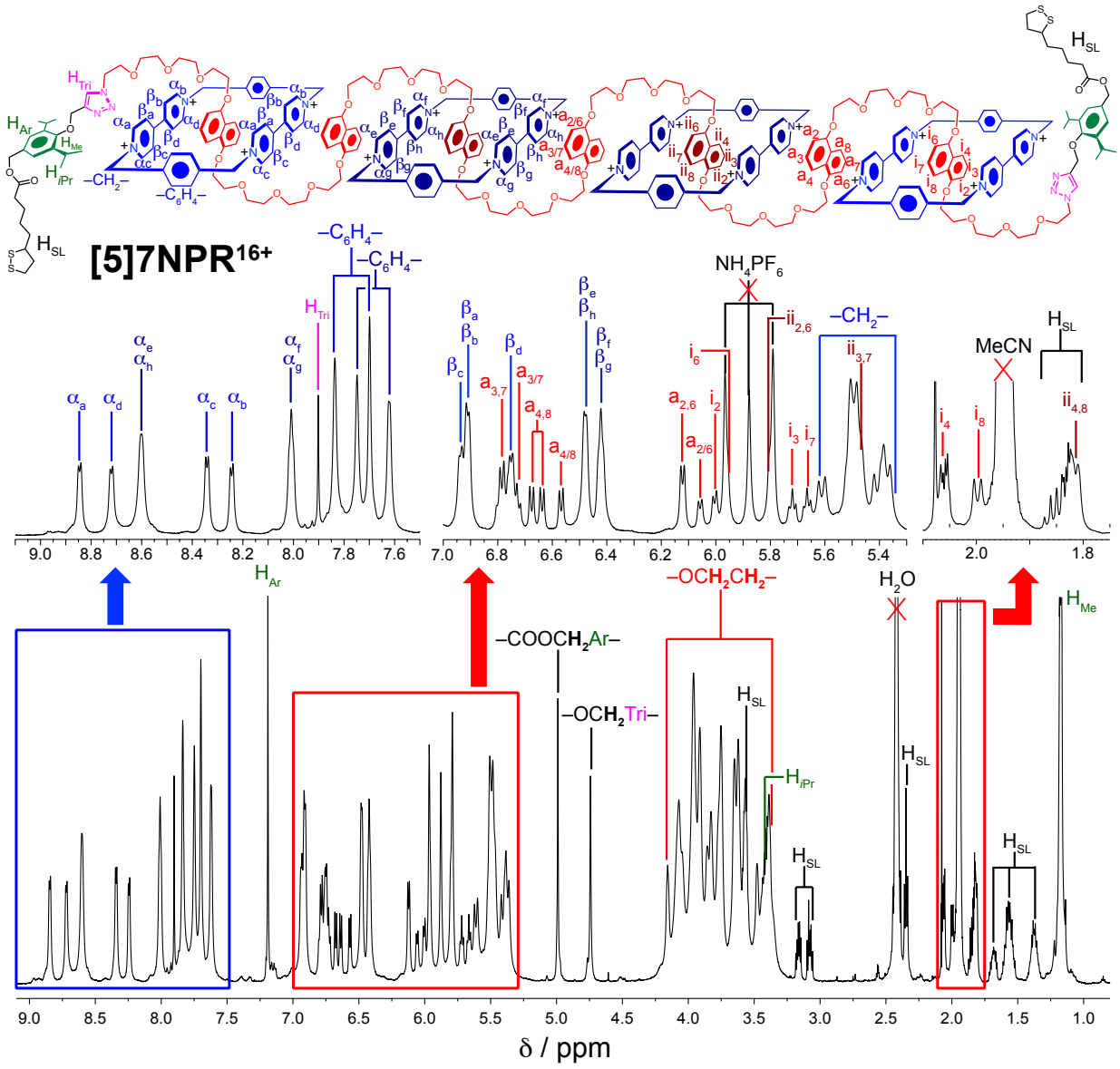

Figure S12. ^{1}H NMR spectrum (600 MHz) of **[5]7NPR**·16PF_6 in CD_3CN at 233 K

Again, we observed that the innermost CBPQT^{4+} resonances are shifted to lower frequency relative to their outermost counterparts, and their lineshapes are slightly broadened by comparison. Since the innermost rings of **[5]7NPR**$^{16+}$ have lower symmetry than that of **[4]5NPR**$^{12+}$, a total of eight α and eight β resonances are expected, but only six are observed because the α and β proton signals of the innermost rings apparently overlap; they have two signals that each integrate for eight protons instead of four signals integrating for four protons.

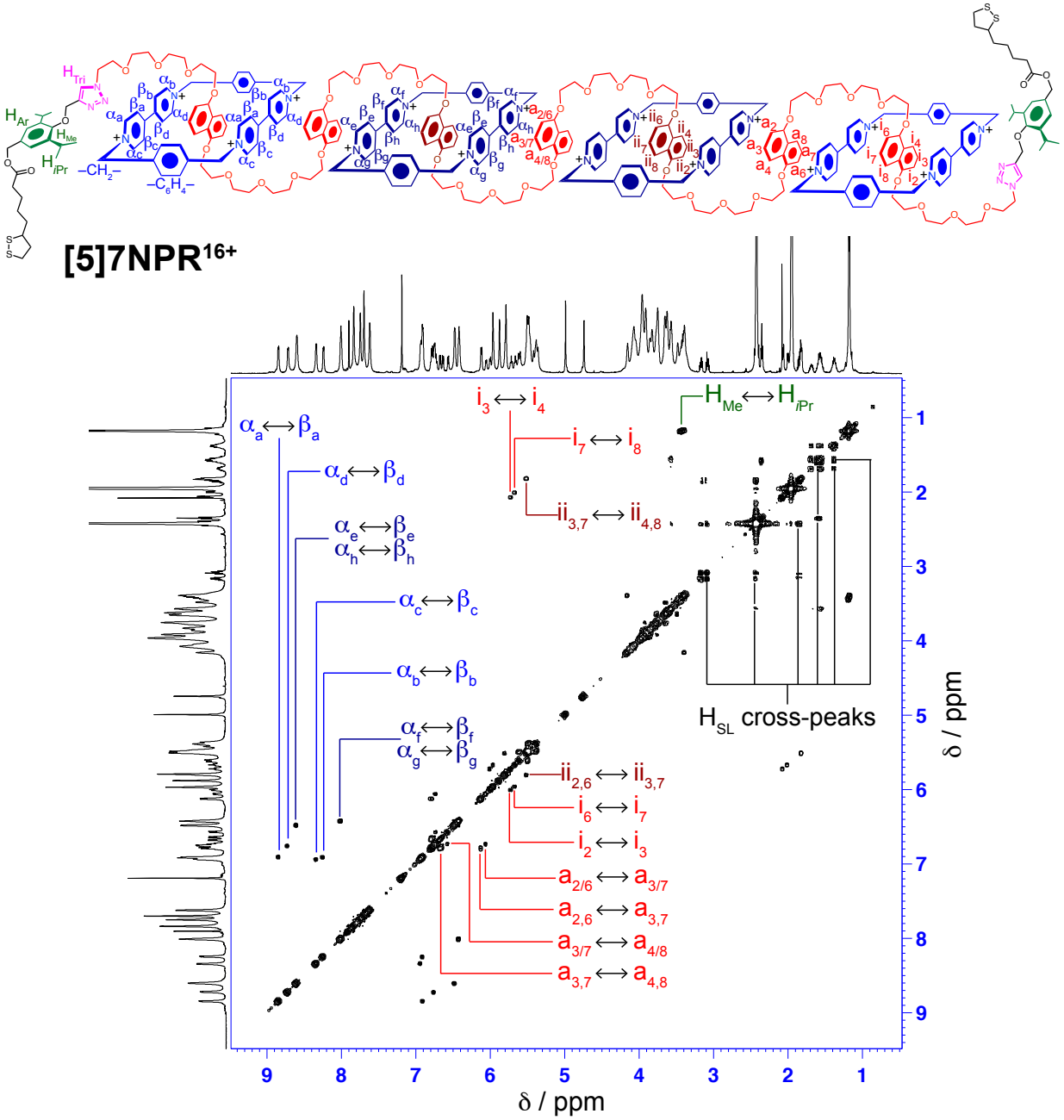

Figure S13. ^{1}H–^{1}H gCOSY spectrum (600 MHz) of **[5]7NPR**·16PF$_6$ in CD$_3$CN at 233 K

All of the expected coupling between α and β ^{1}H signals and 2/6, 3/7, and 4/8 DNP signals were observed in the ^{1}H–^{1}H gCOSY spectrum (Figure S13). The spectrum bears a remarkable similarity to that of **[4]5NPR**·12PF_6, with the main exception being the central alongside DNP unit, whose resonances uniformly appear at slightly lower frequencies than the other alongside DNP resonances, pointing once again to contributions from the continuously stacked folded secondary structure and its shielding effect on the alongside DNP protons.

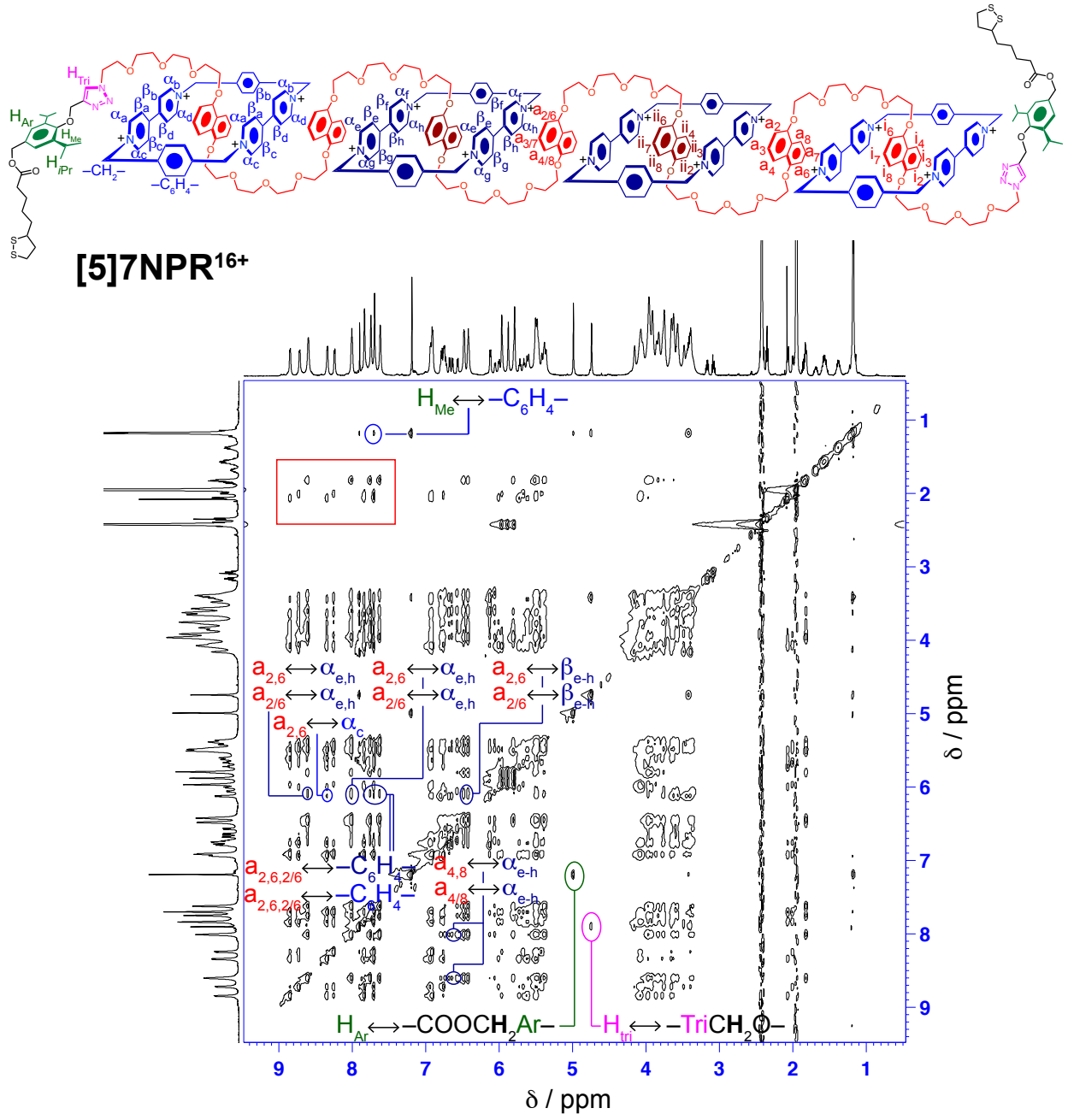

Figure S14. ^{1}H–^{1}H gNOESY spectrum (600 MHz) of **[5]7NPR**·16PF_6 in CD_3CN at 233 K

The ^{1}H–^{1}H gNOESY spectrum (Figure S14) of **[5]7NPR**·16PF$_6$ presents an even stronger case for a folded solution-state secondary structure than that of **[4]5NPR**$^{12+}$ because yet more through-space correlations can be identified between alongside DNP proton resonances and CBPQT^{4+}. It is convenient to use both the 2/6 and the 4/8 resonances of the alongside DNP units as structural probes for **[5]7NPR**$^{16+}$ because all of their signals are isolated and well resolved. For example, a_4, a_8, & $a_{4/8}$ have nOe correlations with the α protons of the inner CBPQT^{4+} rings. All of the $a_{2/6}$ correlations with the innermost CBPQT^{4+} α and β resonances observed in **[4]5NPR**$^{12+}$ are also maintained in **[5]7NPR**$^{16+}$. In addition, we found more rare examples of cross-talk between alongside DNP units and the peripheral CBPQT^{4+} rings by way of the $a_{2,6}$↔α_c and $a_{2,6}$↔–C_6H_4– cross-peaks highlighted in Figure S14.

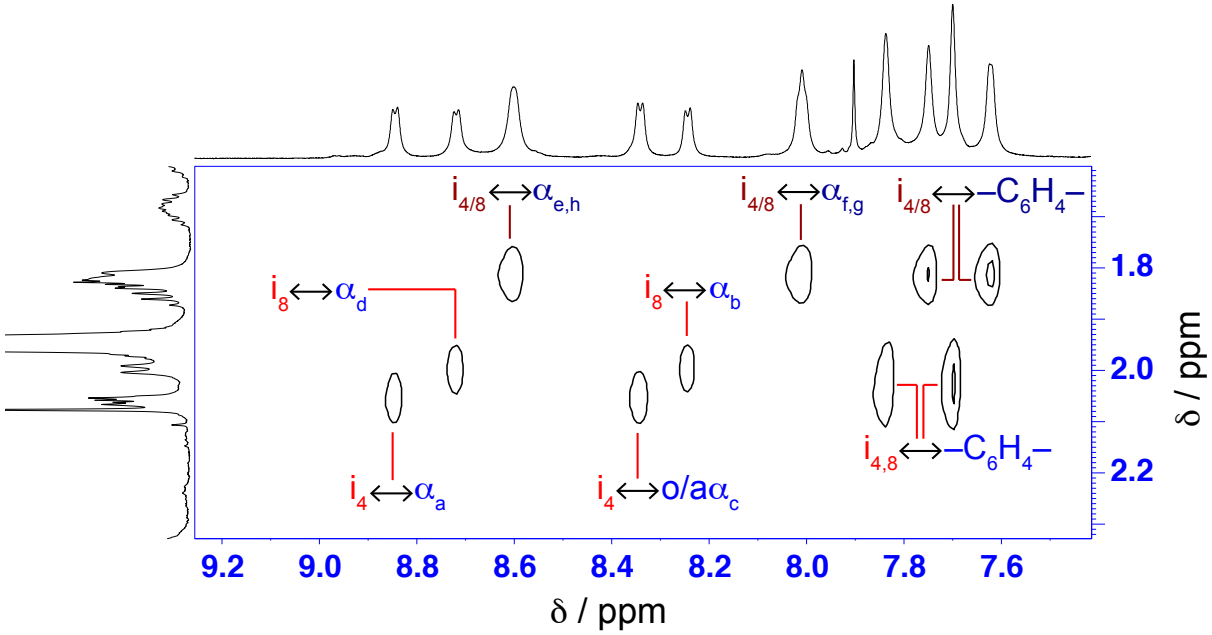

Figure S15 Partial ^{1}H–^{1}H gNOESY spectrum (600 MHz, CD_3CN, 233 K) showing correlations between DNP proton resonances corresponding to i_4, i_8, $ii_{4,8}$ and the α and –C_6H_4– ^{1}H signals of CBPQT^{4+} in **[5]7NPR**·16PF$_6$ (boxed in red in Figure S14)

The partial ^{1}H–^{1}H gNOESY spectrum of **[5]7NPR**$^{16+}$ in Figure S15 is nearly identical to that (Figure S10) of **[4]5NPR**$^{12+}$. See the corresponding description in Section 3D for the significance of these correlations in fully assigning the resonances to their appropriate protons in the molecular structure of the oligorotaxane.

3F. ^{1}H NMR Spectroscopic Analysis of [7]11NPR·24PF$_6$

Although line broadening and signal overlap make it more challenging to assign all of the resonances for **[7]11NPR**$^{24+}$, it is still possible to assign most of the ^{1}H NMR signals of interest without ambiguity, especially for the α and β CBPQT^{4+} protons. The ^{1}H NMR spectrum of **[7]11NPR**·24PF$_6$ is shown in Figure S16. The same labeling scheme carries over from **[5]7NPR**$^{16+}$, except that it becomes necessary to introduce the 'i' prefix to 'alongside' DNP units. In a similar nomenclature to the 'inside' DNP protons, 'alongside' DNP protons with more 'i' prefixes are located further inward, i.e., more distant from the stoppers.

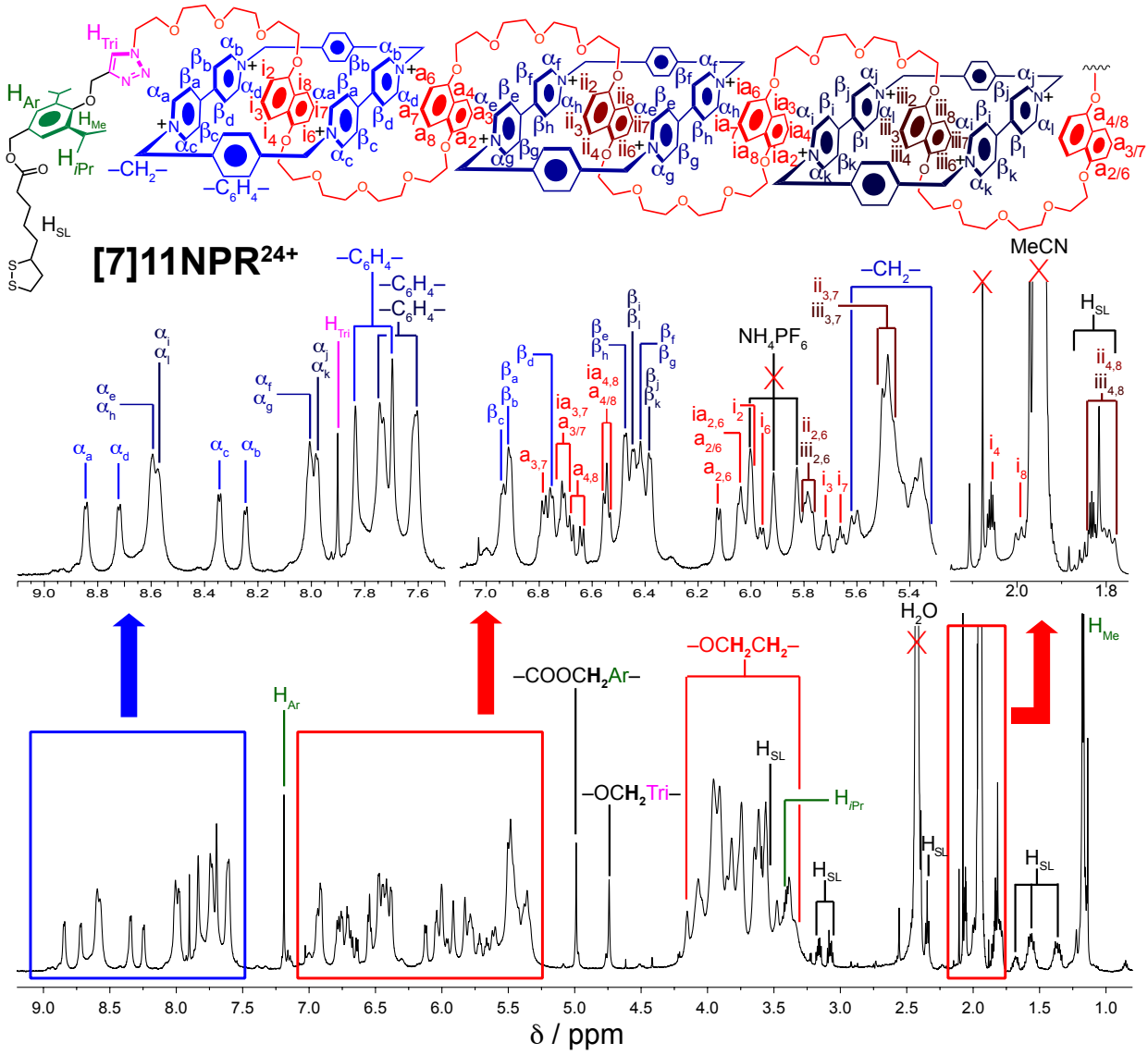

Figure S16. ^{1}H NMR spectrum (600 MHz) of **[7]11NPR**·24PF$_6$ in CD$_3$CN at 233 K

The ^{1}H–^{1}H gCOSY (Figure S17) allowed us to identify the expected α↔β coupling for CBPQT^{4+} resonances and (2,6)↔(3,7) and (3,7)↔(4,8) for DNP. The spectrum is particularly important for identifying the 4 and 8 DNP signals because they are shifted so dramatically as to resonate at the same frequency as the satellite signals for the residual deuterated MeCN solvent. The DNP proton signal i_4, for example, is completely eclipsed by a MeCN satellite so as to be nearly undetectable without the aid of two-dimensional NMR spectroscopy.

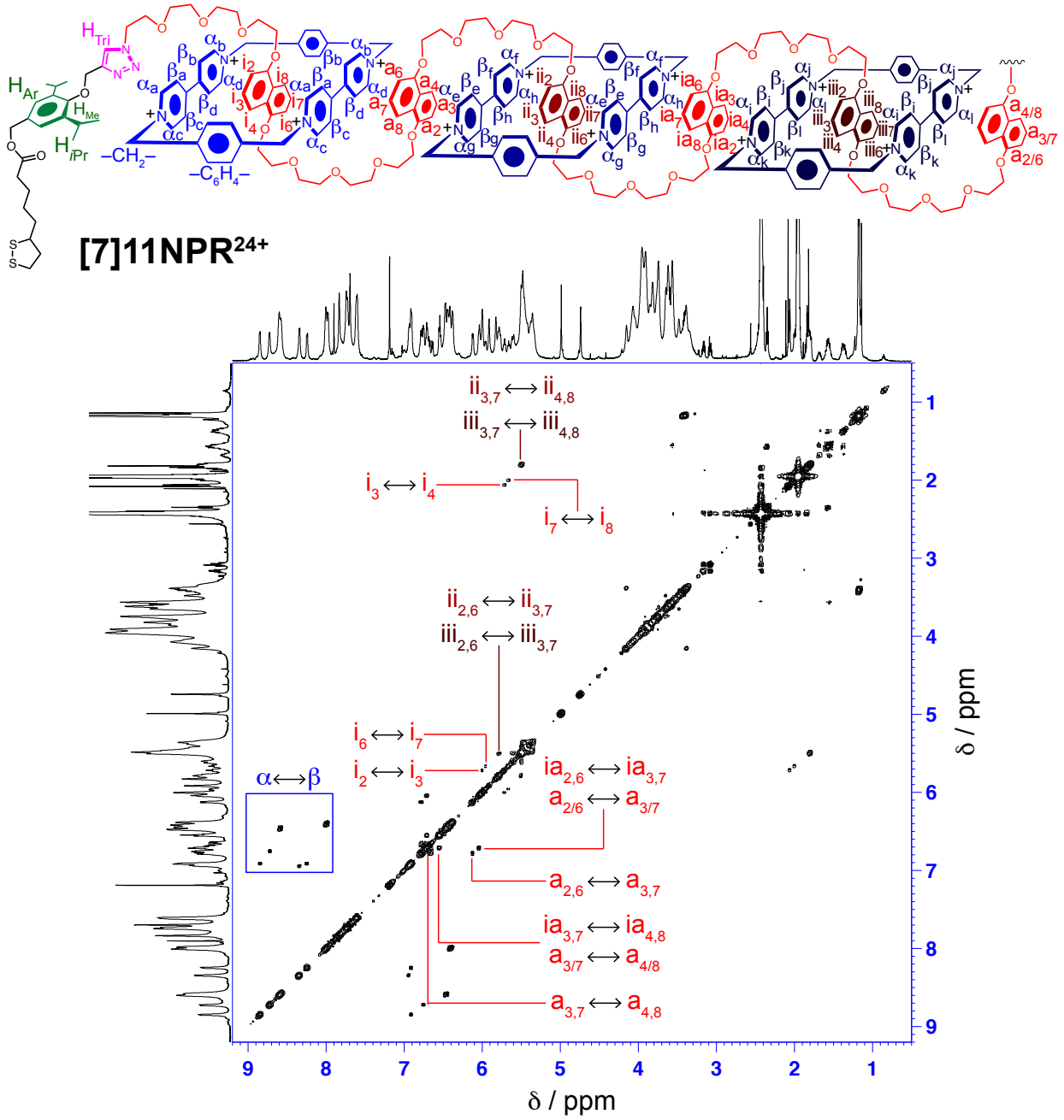

Figure S17. ^{1}H–^{1}H gCOSY spectrum (600 MHz) of **[7]11NPR**·24PF$_6$ in CD_3CN at 233 K

The α and β resonances of the inner CBPQT^{4+} rings of **[7]11NPR^{24+}** have overlapping signals not unlike those of **[5]7NPR^{16+}**. However, in contrast with **[5]7NPR^{16+}**, four of these signals can be observed instead of only two – an observation indicating that the proton resonances for the innermost pair of CBPQT^{4+} rings are once again shifted to slightly lower frequency on account of accumulated aromatic ring-current shift, generated by the interactions at play in the folded secondary structure. This section of the ^{1}H–^{1}H gCOSY spectrum is enlarged in Figure S18 and shows that the four signals are coupled in pairs, providing further support to the same hypothesis.

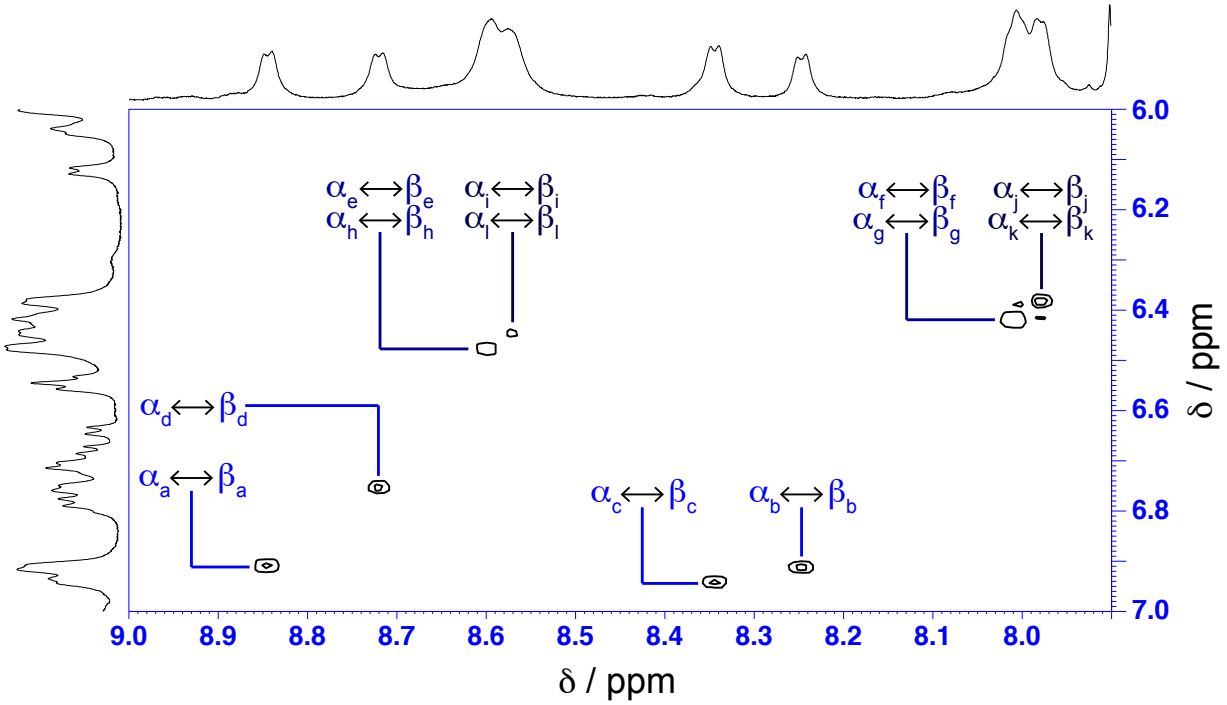

Figure S18. Enlarged section of the ^{1}H–^{1}H gCOSY NMR spectrum of **[7]11NPR**·24PF$_6$ showing the α↔β correlations in the CBPQT^{4+} rings

It is now apparent, after analyzing fully the ^{1}H NMR spectra of oligorotaxanes building up from **[3]3NPR^{4+}** to **[7]11NPR^{24+}**, that the chemical shifts of signals corresponding to the terminal DNP⊂CBPQT^{4+} subcomplex are essentially independent of the oligomer length, while the resonances of the inner subcomplexes gradually shift to lower frequencies as more donor-acceptor stacking sites are iteratively added to the oligorotaxanes. This effect is qualitatively represented by Figure 9 in the main text for the CBPQT^{4+} signals, and quantitatively represented by Figures 10 and 11 in the main text and in the Tables S1 and S2 in Section 3H for all DNP and CBPQT^{4+} signals.

3G. ^{1}H NMR Analysis of [9]15NPR·32PF$_6$

The most synthetically challenging rotaxane of the series, **[9]15NPR**·32PF$_6$, bridges the gap between small molecules and polymers. With a molecular weight of 14693 Da, it comes as no surprise that the ^{1}H NMR spectrum (Figure S19) exhibits line broadening that is characteristic of high molecular weight polymers with their slower tumbling rates. Nevertheless, the majority of the resonances can be identified by the same methods as those described previously.

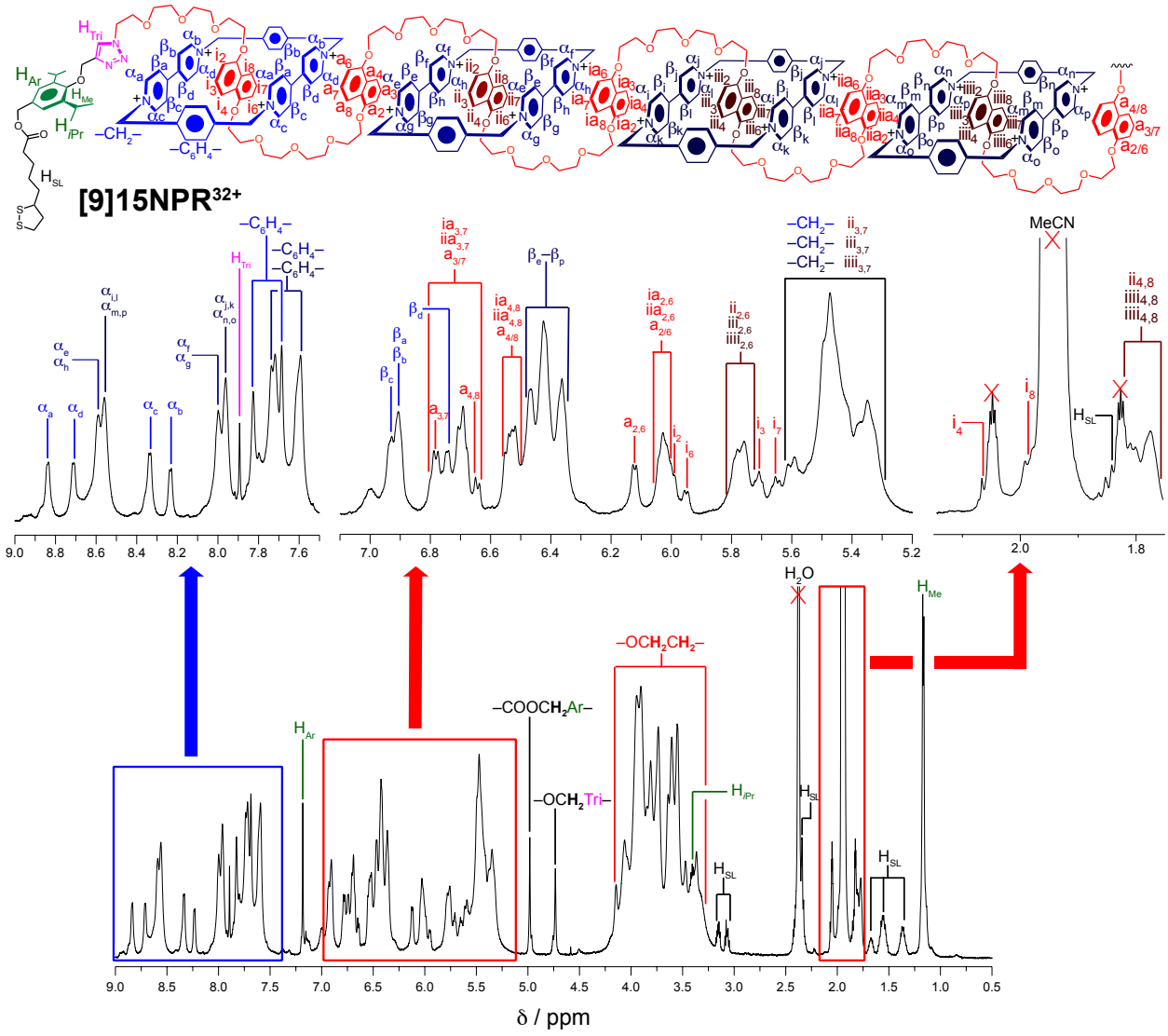

Figure S19. ^{1}H NMR spectrum (600 MHz) of **[9]15NPR**·32PF$_6$ in CD$_3$CN at 233 K

The ^{1}H–^{1}H gCOSY NMR spectrum of **[9]15NPR^{32+}** (Figure S20) made it possible to assign precise frequencies for the purposes of a quantitative analysis of the chemical shifts (Section 3H) to protons with overlapping signals, especially those belonging to included DNP units.

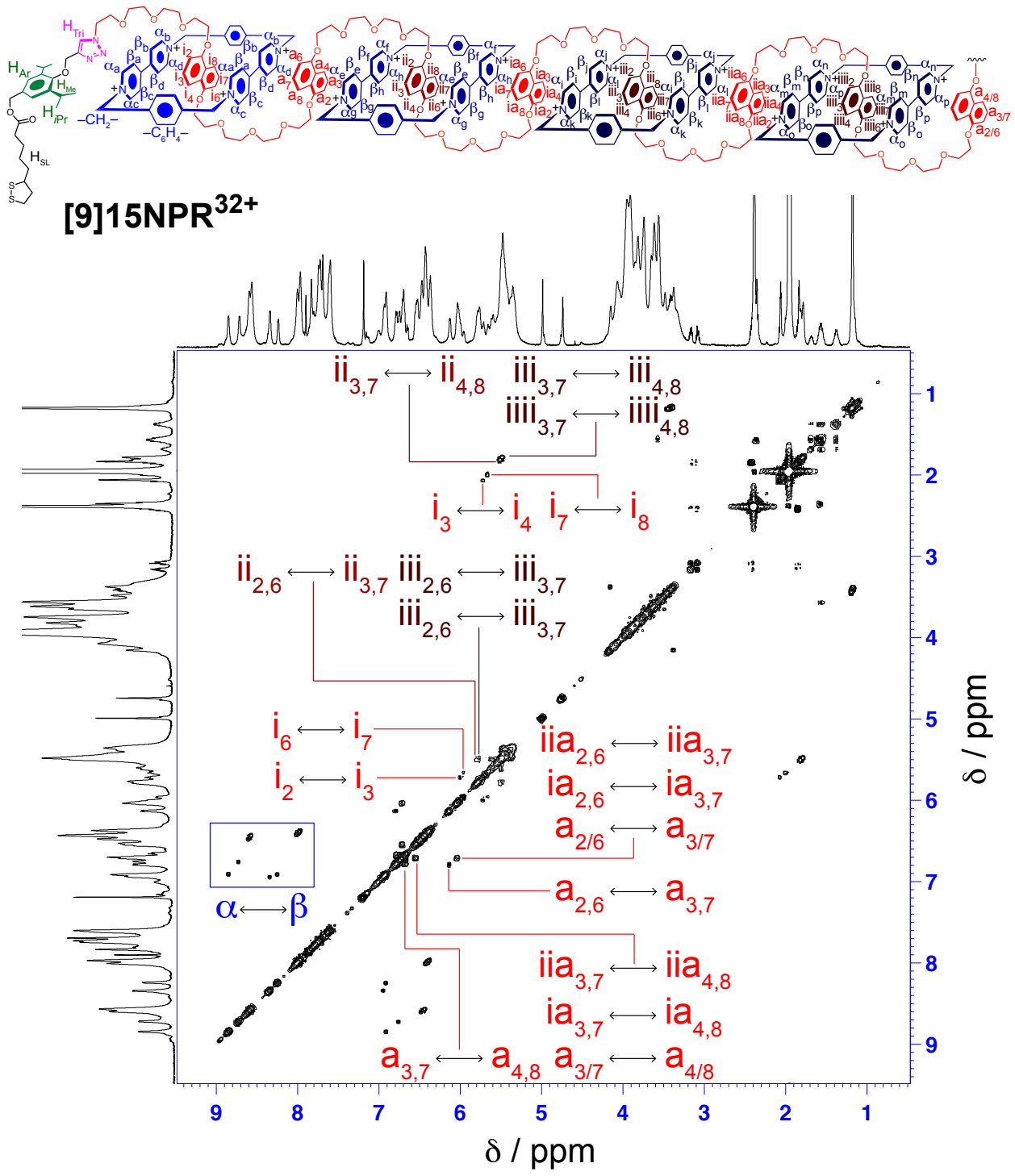

Figure S20. ^{1}H–^{1}H gCOSY spectrum (600 MHz) of **[9]15NPR**·32PF_6 in CD_3CN at 233 K

Although a sufficiently trustworthy trend was established through to **[7]11NPR**$^{24+}$ to assign the signals of **[9]15NPR**$^{32+}$ without the help of nOe spectroscopy, the assignments were still verified

by consulting the ^{1}H–^{1}H gNOESY NMR spectrum. A section of this spectrum, which is shown in Figure S21, highlights the through-space correlations between included DNP protons and $BIPY^{2+}$ units.

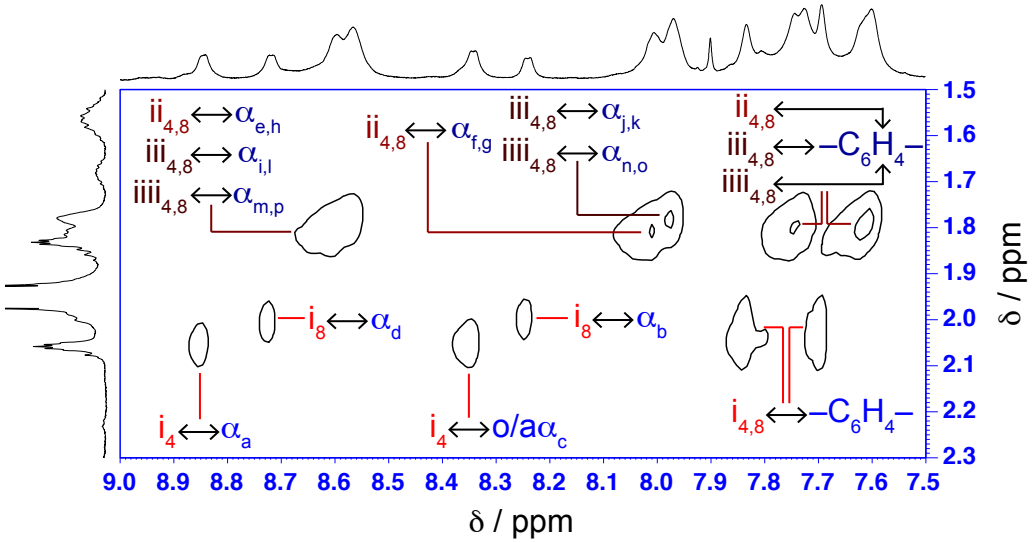

Figure S21 Partial ^{1}H–^{1}H gNOESY spectrum (600 MHz, CD_3CN, 233 K) showing correlations between included DNP protons and the α and $–C_6H_4–$ ^{1}H signals of $CBPQT^{4+}$ rings in **[9]15NPR**·$32PF_6$

Figure S21 underlines the fact that protons in the two sets of $CBPQT^{4+}$ rings at the innermost sites of the rotaxane resonate at equal frequencies, indicating that the accumulated aromatic ring-current shifts are saturated. In other words, adding more repeat units to the oligomers is expected to have a minimal effect on the observed chemical shifts.

3H. Quantitative Analysis of Chemical Shifts in the Oligorotaxanes

The chemical shifts for all of the DNP and $BIPY^{2+}$ proton environments were tabulated for each oligorotaxane and the results are presented in Table S1 (for DNP protons) and Table S2 (for $BIPY^{2+}$ protons). Certain DNP signals were averaged for the sake of brevity in cases where related proton environments (i_2 and i_6 or i_3 and i_7, for example) resonated at slightly different frequencies. The values in Tables 1 and 2 can be used to visualize the trends in chemical shifts as repeat units are added to the oligomers (see Figure 10 in the main text) and to obtain values for Δδ (Figure 11 in the main text) by subtracting them from the appropriate chemical shifts of the corresponding dumbbell or cyclophane proton at 233K in CD_3CN.

Table S1. The Chemical Shifts (δ) of DNP Protons in Each of the Oligorotaxanes **[2]1NPR^{4+}**–**[9]15NPR^{32+}** at 233 K in CD_3CN

Proton	δ (ppm)					
	[2]1NPR^{4+}	**[3]3NPR^{8+}**	**[4]5NPR^{12+}**	**[5]7NPR^{16+}**	**[7]11NPR^{24+}**	**[9]15NPR^{32+}**
Included DNP						
$i_{2,6}$	6.15	6.01[a]	5.98[a]	5.98[a]	5.97[a]	5.97[a]
$i_{3,7}$	5.86	5.71[a]	5.69[a]	5.69[a]	5.68[a]	5.68[a]
$i_{4,8}$	2.23	2.06[a]	2.03[a]	2.02[a]	2.02[a]	2.02[a]
$ii_{2,6}$			5.81[b]	5.79	5.79	5.79[c]
$ii_{3,7}$			5.52[b]	5.51[c]	5.49[c]	5.49[c]
$ii_{4,8}$			1.83[b]	1.81[c]	1.80[c]	1.80[c]
$iii_{2,6}$					5.77	5.75[c]
$iii_{3,7}$					5.48[c]	5.48[c]
$iii_{4,8}$					1.78[c]	1.80[c]
$iiii_{2,6}$						5.75[c]
$iiii_{3,7}$						5.47[c]
$iiii_{4,8}$						1.77[c]
2/6 Average		**6.01**	**5.90**	**5.89**	**5.84**	**5.81**
3/7 Average		**5.71**	**5.61**	**5.58**	**5.55**	**5.53**
4/8 Average		**2.06**	**1.96**	**1.91**	**1.87**	**1.85**
Total Average	**4.75**	**4.59**	**4.48**	**4.46**	**4.42**	**4.40**
Alongside DNP	**[2]3NPR^{4+}** [d]					
$a_{2,6}$	6.32		6.12	6.12	6.12	6.12
$a_{3,7}$	7.03		6.79[a]	6.78[a]	6.78[a]	6.77[a]
$a_{4,8}$	7.18		6.66[a]	6.65[a]	6.65[a]	6.66[a]
$ia_{2,6}$					6.04	6.04[c]
$ia_{3,7}$					6.71	6.70[c]
$ia_{4,8}$					6.54[a]	6.55[c]
$iia_{2,6}$						6.03[a]
$iia_{3,7}$						6.70[a,c]
$iia_{4,8}$						6.53[a,c]
$a_{2/6}$		6.22		6.05	6.03	6.01
$a_{3/7}$		6.86		6.72	6.70	6.68[c]
$a_{4/8}$		6.78		6.56	6.53	6.52[c]
2/6 Average	**6.52**	**6.22**	**6.12**	**6.09**	**6.06**	**6.05**
3/7 Average	**7.03**	**6.86**	**6.79**	**6.75**	**6.73**	**6.71**
4/8 Average	**7.18**	**6.78**	**6.66**	**6.61**	**6.57**	**6.56**
Total Average	**6.91**	**6.62**	**6.52**	**6.48**	**6.46**	**6.44**

[a]Reported chemical shift is an average of two well-resolved signals. [b]Protons $i_{2/6}$, $i_{3/7}$, and $i_{4/8}$ are listed under entries $ii_{2,6}$, $ii_{3,7}$, and $ii_{4,8}$, respectively, because they are located in the innermost inclusion complex of **[4]5NPR^{12+}**. [c]Chemical shifts of overlapping signals were discerned by inspection of the ^1H-^1H gCOSY NMR spectrum. [d]**[2]3NPR^{4+}** is introduced to obtain a value for alongside DNP units in a two-component rotaxane, since **[2]1NPR^{4+}** has no alongside units.

Table S2. The Chemical Shifts (δ) of $BIPY^{2+}$ Protons in Each of the Oligorotaxanes **[2]1NPR^{4+}**–**[9]15NPR^{32+}** at 233 K in CD_3CN

Proton	δ (ppm)					
	[2]1NPR^{4+}	**[3]3NPR^{8+}**	**[4]5NPR^{12+}**	**[5]7NPR^{16+}**	**[7]11NPR^{24+}**	**[9]15NPR^{32+}**
α BIPY^{2+}						
α_a	8.96	8.88	8.84	8.84	8.84	8.84
α_b	8.53	8.27	8.24	8.24	8.24	8.23
α_c		8.39	8.34	8.33	8.34	8.33
α_d		8.75	8.72	8.71	8.71	8.71
$\alpha_{e,h}$			8.62	8.60	8.59	8.59
$\alpha_{f,g}$			8.02	8.00	8.00	8.00
$\alpha_{i,l}$					8.57	8.56
$\alpha_{j,k}$					7.97	7.96
$\alpha_{m,p}$						8.56
$\alpha_{n,o}$						7.96
Outer Rings	8.75	8.57	8.54	8.53	8.53	8.53
Inner Rings			8.32	8.30	8.28	8.27
Average	**8.75**	**8.57**	**8.46**	**8.45**	**8.41**	**8.37**
β BIPY^{2+}						
β_a	7.35	6.94	6.91	6.90	6.90	6.90
β_b	7.13	6.94	6.91	6.90	6.90	6.90
β_c		6.98	6.93	6.93	6.93	6.93
β_d		6.79	6.75	6.74	6.74	6.74
$\beta_{e,h}$			6.50	6.47	6.47	6.47
$\beta_{f,g}$			6.44	6.41	6.40	6.41
$\beta_{i,l}$					6.44	6.43
$\beta_{j,k}$					6.37	6.36
$\beta_{m,p}$						6.43
$\beta_{n,o}$						6.36
Outer Rings	7.24	6.91	6.88	6.83	6.83	6.83
Inner Rings			6.47	6.44	6.42	6.41
Average	**7.24**	**6.91**	**6.74**	**6.72**	**6.64**	**6.59**

4. References

(S1) M. Asakawa, W. Dehaen, G. L'abbé, S. Menzer, J. Nouwen, F. M. Raymo, J. F. Stoddart, D. J. Williams, *J. Org. Chem.,* 1996, **61**, 9591–9595.

(S2) C. J. Bruns, S. Basu, J. F. Stoddart, *Tetrahedron Lett.*, 2010, **51**, 983–986.

(S3) S. Basu, A. Coskun, D. C. Friedman, M. A. Olson, D. Benítez, E. Tkatchouk, G. Barin, J. Yang, A. C. Fahrenbach, W. A. Goddard III, J. F. Stoddart, *Chem. Eur. J.*, 2011, **17**, 2107–2119.

(S4) R. S. Stoll, D. C. Friedman, J. F. Stoddart, *Org. Lett.*, 2011, **13**, 2706–2709.

(S5) D. B. Amabilino, P.-L. Anelli, P. R. Ashton, G. R. Brown, E Córdova, L. Godínez, W. Hayes, A. E. Kaifer, D. Philp, A. M. Z. Slawin, N. Spencer, J. F. Stoddart, M. S. Tolley, D. J. Williams, *J. Am. Chem. Soc.*, 1995, **117**, 11142–11170.